ADAPTATION OF THE AUGMENTED SPACE METHOD FOR THE COHERENT POTENTIAL AND CLUSTER COHERENT POTENTIAL APPROXIMATIONS FOR MAGNETIC ALLOYS

by

ARUN KUMAR MISHRA

DEPARTMENT OF PHYSICS
INDIAN INSTITUTE OF TECHNOLOGY, KANPUR

APRIL, 1989

ADAPTATION OF THE AUGMENTED SPACE METHOD FOR THE COHERENT POTENTIAL AND CLUSTER COHERENT POTENTIAL APPROXIMATIONS FOR MAGNETIC ALLOYS

A Thesis Submitted
in Partial Fulfilment of the Requirements
for the Degree of
DOCTOR OF PHILOSOPHY

by

ARUN KUMAR MISHRA

to the

DEPARTMENT OF PHYSICS
INDIAN INSTITUTE OF TECHNOLOGY, KANPUR
APRIL, 1989

PHY-1989-D-MIS-ADA

TO

MY DARLING

CERTIFICATE

This is to certify that the work of this thesis entitled : ADAPTATION OF THE AUGMENTED SPACE METHOD FOR THE COHERENT POTENTIAL AND CLUSTER COHERENT POTENTIAL APPROXIMATIONS FOR MAGNETIC ALLOYS has been carried out by ARUN KUMAR MISHRA under my supervision. No part of this work has been submitted elsewhere for a degree.

Abhijit Mookerjee
Professor
Department of Physics
Indian Institute of Technology
Kanpur 208016, INDIA

April, 1989

ACKNOWLEDGEMENTS

I gratefully acknowledge the able guidance and constant help of Professor Abhijit Mookerjee throughout my Ph.D programme. It is almost impossible to list out what all I got from him. In short,working with him has been a pleasant and memorable experience of my life.

My sincere thanks are due to Prof.M.Yussouff, Prof.A.K.Majumdar, Dr.V.A.Singh and Dr.R.Prasad for their expert comments and wise suggestions from time to time.

I am also thankful to my senior collegue Dr.P.K.Thakur for his help in computational work. I also gained from various discussions with him as also from my friend Mr.S.S.A.Razee. Besides, the latter, help of several other friends at I.I.T.Kanpur, Mr.S.S.Rajput, Mr.Biplab Ganguly, Mr.Amit Sircar, Ms.Samita Bardhan to name a few, is gratefully ackowledged.

I am grateful to the University Grants Commission, New Delhi and D.S.College, Katihar (Bihar) for financial support in the form of a teacher fellowship under its

undergraduate development scheme.

Lastly, I must also thank my family members who stood by me and encouraged me to complete this work.

Arun Kumar Mishra

CONTENTS

SYNOPSIS

This thesis entitled "ADAPTATION OF THE AUGMENTED SPACE METHOD FOR THE COHERENT POTENTIAL AND CLUSTER COHERENT POTENTIAL APPROXIMATIONS FOR MAGNETIC ALLOYS" submitted by Arun Kumar Mishra to the Department of Physics, Indian Institute of Technology, Kanpur in partial fulfilment of the requirements of the Ph.D. degree

The problems of electronic states and electronic transport in disordered alloys are a matter of interest for a long time now both for theoretical and experimental physicists. For more than two decades now, the Coherent Potential approximation (CPA) remains one of the main tools in the hands of theoretical physicists working in the area of electronic structure of disodered alloys. In the simplest case of CPA calculation for random binary alloy A_cB_{1-c} where c is the concentration of A in B, the site energies are taken to be random (diagonal disorder) and the overlap integrals are assumed to be non-random i.e there is no off-diagonal disorder. In this case correlated scattering from two or

more sites are ignored. Thus it is known as single site COHERENT POTENTIAL APPROXIMATION (1CPA).

The need to go beyond the single site was felt for a long time. In CHAPTER II, A self-consistent Cluster CPA formalism to obtain a configurationally averaged Green function is discussed. This formalism is based on AUGMENTED SPACE method introduced by Mookerjee (1973). In the self-consistent cluster generalisation (CCPA) of 1CPA, statistical clustering effects and off-diagonal disorder over finite cluster sizes are successfully taken into account. Besides, it preserves the Herglotz analytic properties of the Green function which is essential for getting physically meaningful results.

In all earlier applications of the Augmented Space approach the underlying potential was taken as known. In this chapter the Augmented Space approach is generalised to include cases where the potential itself has to be generated self-consistently. The work then involves two self-consistency loops - the one for generation of the Coherent Potential, given the random potential and then regeneration of the random potential itself. This generalisation is the principal contribution of the thesis.

The Augmented Space method coupled with the

Recursion method introduced by Haydock (1972) enables us to work on a realistic three-dimensional lattices. The Recursion method, discussed in CHAPTER III, is now a well established means of solving the Schrödinger equation for a system in which local interactions dominate. The local density of states and related quantites are calculated from the continued fraction expansions generated through the application of the recursion method. In this chapter the various terminator schemes have also been discussed. The density of states of pure Ni (the host in the system) is generated from the programmes modified from the Cambridge Recursion Library (1984).

In chapter IV, an application of the above formalism is made. The electron correlation in narrow energy bands of transition metals is also dealt with. The system is Ni rich $Ni_{1-c}Fe_c$ alloy in the magnetic states. The usual tight-binding Hamiltonian incorporates an extra term which accounts for the on-site Coulomb repulsion of the electrons. It is this term in the Hamiltonian which has to be generated self-consistently. This is the so called Anderson-Hubbard Hamiltonian which is used to consider the spin fluctuations and moment formation on alloying of the transition metal Ni with Fe. Another feature of this work is that, till now, the Augmented Space method was used only for the density of states calculations and other response

functions of the Green function like residual conductivity or optical conductivity etc. In this work local magnetisation is also considered, apart from the density of states calculations. The CPA and Cluster CPA results are obtained and compared. In low concentration regimes,i.e the so called impurity regimes,the CPA fails to give good results,as in all earlier applications. The cluster generalisation gives correction in the right direction.

In Chapter V, the achievents and shortcomings of the present work is discussed. Some of the problems in the field is also suggested.

LIST OF FIGURES

CHAPTER I

INTRODUCTION

The problem of electronic states in disordered metallic alloys received the attention of solid state physicists with the application and extension of the pioneering work on the Coherent Potential Approximation (CPA) by Soven (1967), Kirkpatrick *et. al.* (1970), Stocks *et al* (1971) etc. Soven introduced the idea of a complex site energy (or potential) which characterises the effect of the random environment within a meaningful picture. This potential (called the Coherent Potential) was determined self-consistently from the requirement that a particular configuration immersed in the effective medium (the mean field) yields no extra scattering on the average.

The validity of the single site CPA theory has been accepted in a large class of systems after its successful application to various model Hamiltonians suitable for disordered metallic alloys. Kirkpatrick *et al* (1970) made its application to Ni rich Ni_{1-c} Cu_c alloy and Stocks *et al*

(1971) did the same for Cu rich Cu_{1-c} Ni_c alloys for studying the electronic density of states. Their results were in good agreement with the experimental data reported by Seib and Spicer (1970) and Huffner *et al* (1973).

Single site CPA theory has, however, the following drawbacks:

i) It takes into account only single site scattering and correlated scattering from clusters is not accounted for

ii) the effect of potential fluctuations is suppressed while doing such an average

iii) the off diagonal disorder in the tight-binding Hamiltonians cannot be properly accounted for

So, the need was felt to go beyond the single site approximation and also incorporate off-diagonal disorder. Nickel and Krumhansl (1971) tried to make such a generalisation using a method based on the corrected cumulant expansion to find electronic density of states of an one-dimensional model of an alloy. Butler (1972, 1973) calculated the real and imaginary parts of the Green function using a self-consistent cluster method. Without going into the details of these methods, it will suffice to say that

both were attempts to improve the CPA by going beyond the single site approximation through making application to one-dimensional tight binding models. This generalisation posed severe analytic problems, such as multivalued, discontinuous and negative density of states in certain energy regions.

Haydock *et al* (1972), Mookerjee (1973 a,b), Muller-Hartman (1973) and Mills and Ratanavararaksa (1978) pointed out that for any real potential function, the Green function must obey certain mathematical properties called the Herglotz properties. A complex function f(z) was defined as Herglotz if

i) Im $f(z) \leq 0$ for Im $z>0$
ii) Singularities of f(z) lie on the real axis, and
iii) $f(z) \longrightarrow 1/E$ as $E \longrightarrow \infty$ (where $z = E + i0^{+}$)

In order to get physical results Herglotzicity has to be retained in any approximation to the Green function. The basic fault with a majority of the extensions of the CPA proposed in late 60's and early 70's was that they led to approximate Green functions which were not Herglotz. It has to be borne in mind that in the development of a theory which includes scattering from clusters, short ranged order,

off-diagonal disorder or the effects of positional disorder, Herglotz property must be inherently retained.

Some other attempts at generalisations led to the Molecular Coherent Potential approximation (MCPA) proposed by Tsukada (1969) and Butler (1973), Embedded Cluster method (ECM) discussed by Inglesfield (1981) and Baraff *et al* (1986) and Travelling Cluster approximation proposed by Mills (1978).

Mookerjee (1973a, b, 1975 a,b,c) introduced a formalism called the Augmented Space formalism (ASF) to calculate configuration average of a general function of many random variables. He was able to incorporate scattering effects from statistically coupled sites in finite size clusters and also off-diagonal disorder in a self consistent manner.

Before understanding the Augmented Space method, we have to know what configuration averaging implies and why we need to configuration average a quantity ; as also what is it that we should average. In the study of disordered systems, configuration averaging is a necessary requirement. The potentials which describe a disordered solid are characterised by random parameters: random in space as in quenched disordered solids or random in time as in thermally disordered systems, for example, electrons in contact with a

phonon bath. There are examples where both spatial and temporal disorders are involved for example, dirty alloys (Mooij systems) at high temperatures A particular realisation of these parameters, either in a given sample or at an instant of time is what we refer to as the configuration of the system.

To understand why we must take resort to configuration averaging, we take an example, say of a crystalline, substitutionally random binary alloy, in which the regular lattice sites are randomly occupied by A or B type atoms. Cu-Ni is a good example. At T= 0, the randomness is quenched and spatial, and may be described by a set of random occupation variables n_i which takes values 0 and 1 only and thereby determines, whether a site labelled by i is occupied by a A or a B type of atom. A configuration is determined by a particular assignment of 0's and 1's to the sequence $\{n_i\}$. Any one sample therefore corresponds to a particular configuration. There can be in all 2^N different configurations for a sample containing N atoms. This is a very large number for macroscopic systems. When an experimentalist talks about the characteristics of the samples he measures, he wants average trends among his samples; he has no interest in the variations between the large number of configurations. If the fluctuations of a characteristics from sample to sample(i.e. from configuration

to configuration) is negligible compared to the mean, then it is the configuration average which should be compared with experimentally determined characteristics.

It is clear from above why configuration averaging is required. Also, it is the physically measured property which should be configurationally averaged: the density of states or the response functions rather than the Hamiltonian or self-energies; the diffusion probabilities rather than wave functions. Anderson (1969) has tried to explain some of the anomalous results on the nature of the spectrum of random tight binding Hamiltonians, which were proposed at that time, based on configuration averaging. That is why, Green function techniques are favoured for the study of disordered systems rather than the Schrödinger equation approach.

Configuration averaging is a valid procedure only when the probability distribution of the property under consideration is sufficiently well behaved so that the mean dominates over the higher moments. The intensity of star light transmitted through layered media with randomly varying refractive indices studied by Chandrasekhar (1960) and the closely related problem of the resistance of disordered chain is an example. Kumar and coworkers (1985, 1986) have shown that the variance of the resistance of a disordered chain diverges much faster than its mean as the length of the chain

increases. It is, therefore, not meaningful to talk in terms of the average resistance of a very long disordered chain.

Now something about spatial ergodicity. For a very large system, in the limit of infinite size, all possible environments may be achieved even in a single sample. The Fig 1.1 will illustrate this idea.

A global probe can sample all possible environments in the samples weighted with appropriate probabilities. A global property is thus automatically configurationally averaged, even if it refers to a single sample. Thus, a spatially global probe samples the entire configuration space just as in statistical mechanics, the entire phase space is sampled by a dynamically evolving system. Hence the name 'spatial ergodicity'. Such global properties need not be configurationally averaged all over again.

In § 2.2 in Chapter II, we will discuss in detail how to configuration average any physical quantity in a simple tight binding model for a substitutionally disordered binary alloy. Response functions, like optical conductivity, residual resistivity etc. can be configurationally averaged.

Till now, the Augmented Space method has been used for parametrised Hamiltonions alone. For this it has come under criticism . The main aim of the present work is to

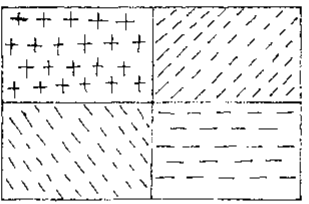

Fig. 1.1 Representation of different environments within a sample. For $n \longrightarrow \infty$, all environments are realised.

extend Augmented Space Formalism to cases where the potential itself has to be found self consistently. One such example is a system with a potential given by

$$V(\vec{r}) = V_0(\vec{r}) + \alpha\,[\rho(\vec{r})]^{1/9} \qquad (1.1)$$

where the second term is the exchange correlation potential with

$$\rho(\vec{r}) = -\frac{1}{\pi}\int_{-\infty}^{E_F} \mathrm{Im} \langle G(\vec{r},\vec{r},E)\rangle_{av}\, dE \qquad (1.2)$$

$$\text{and} \quad \langle G(E)\rangle_{av} = [\,EI-\tilde{H}\,]^{-1} \qquad (1.3)$$

Thus, $\rho(\vec{r})$ can be evaluated self-consistently by the use of equations (1.2) and (1.3).

We shall, however, choose a simpler case, which is nevertheless of considerable interest. We shall study a magnetic alloy within the framework of the Hartree-Fock approximation. The spin dependent Hamiltonian is itself dependent on the number of up($\uparrow$) or down ($\downarrow$) electrons and hence has to be obtained self consistently.

In Chapter II the Augmented Space Formalism is introduced with its mathematical formulations and it is shown how it can be used both for CPA and cluster CPA.

Chapter III deals with the Recursion method. It also incorporates the different terminator schemes and application to d-states. Chapter IV deals with electron correlation in narrow energy bands. It also discusses how the Hubbard model is utilised for the study of spin fluctuation and moment formation in Ni rich $Ni_{1-c}Fe_c$ systems for different Fe concentrations. Finally, magnetic moment results obtained theoretically are compared with the experimental results.

CHAPTER II

THE AUGMENTED SPACE METHOD

2.1 INTRODUCTION

An electron moving in a disordered solid experiences random potentials at the lattice positions. The Hamiltonian thus has a very large number of configurations. The disorder is characterised by a set of Hamiltonian parameters, which are random variables and obey some probability distribution. The description of such systems, should be from a statistical point of view and the physical properties of the system may, for instance, be described through configuration averaging of the physical observables.

The Augmented Space formalism (ASF) is a technique of configuration averaging where configuration fluctuations are systematically taken into account. The formalism is formally *exact* but, for practical calculations, approximations preserving constraints of physical origin may be generated. The ASF was first introduced by Mookerjee

(1973a,1973b) and later on Kaplan and Gray (1976,1977) provided a detailed exposition. It has been successfully utilised for averaging quantities like one particle Green functions and response functions related to two particle Green functions, particularly when we have to go beyond the single site approximations (i.e beyond the CPA) and have to include clustering effects, large off-diagonal disorder, short range order *etc*.

Previously, the formulations utilizing the ASF concentrated on model or parametrised Hamiltonians. The density functional approach leads to Hamiltonians self consistently derived from the particle density. The aim of this work is to develop such a formalism and apply it to magnetic systems like Ni rich Ni-Fe alloys.

2.2 MATHEMATICAL FORMULATION OF ASF AND ITS APPLICATION TO MODEL SYSTEMS

In his various communications Mookerjee (1973 a,b; 1975 a,b,c) has worked out the detailed mathematics of the ASF. Here we discuss the main points of the formalism. Our formulation will be in a tight binding basis.

In a substitutional system the lattice sites are

randomly occupied by the atoms of the type say A,B,C .etc. So in a binary alloy the site energy ε_i is a random variable which takes values ε_a or ε_b depending upon whether the site is occupied by an A or B type of atom respectively. The Hamiltonian involves a random occupation variable n_i, defined to take the value 0 or 1 according to the occupation of site i by an A or B type of atom. A set of values taken up by the random occupation variable $\{n_i\}$ is called a *configuration*. Assuming no correlation between these random variables, we can define their distribution function in the form

$$P(\{n_i\}) = \prod_i p_i(n_i) \qquad (2.1)$$

where $p_i(n_i)$ is the probability density of the individual variables. This assumption ignores short range order due to chemical clustering effects. Kaplan and Gray (1981) have considered the more general case of such dependent variables within a Markovian short ranged order model.

Haydock (1972) suggested that the probability density $p_i(n_i)$ satisfies $p_i(n_i) \geq 0$ and $\int p_i(n_i)dn_i = 1$. Thus the probability density $p_i(n_i)$ shares with the density of states, the property of positive definiteness and integrability. Physically too, both give the number (or fraction) of states in a range $\Delta\varepsilon$ around the energy value ε.

Mookerjee (1973) introduced a hypothetical space ϕ_ι corresponding to a random variable n_ι such that a basis set $\{|f_n^\iota\rangle\}$ and an operator $M^{(\iota)}$ on it characterised the random distribution of n_ι through the relation

$$p(n_\iota) = -(1/\pi)\,\mathrm{Im}\left\langle f_o^\iota \middle| \left[(n_\iota + i\delta)I - M^{(\iota)}\right]^{-1} \middle| f_o^\iota \right\rangle \qquad (2.2)$$

Thus the quantities $|f_n^\iota\rangle$, $M^{(\iota)}$ and $p(n_\iota)$ are respectively analogous to eigen vectors, Hamiltonian and density of states. Subsequently Mookerjee (1975) described $|f_n^\iota\rangle$ as the disorder field in analogy with a fermion/boson field and was able to give a diagrammatic representation of it in a way similar to Feynman diagrams for fermions or bosons. Knowing the Hamiltonian, it is straightforward to find the density of states; however, in our case we have the reverse problem at hand : for a given probability distribution we have to find out an operator $M^{(\iota)}$ corresponding to $p(n_\iota)$ such that equation (2.2) is satisfied. Here $|f_o^\iota\rangle$ is a specially chosen member of the orthonormal basis $\{|f_n^\iota\rangle\}$ in ϕ_ι.

The problem can be handled in a way analogous to the continued fraction expansion of Green functions in the Recursion method (Haydock, 1972). One has to try to write the probability density $p(n_\iota)$ in the form of a convergent

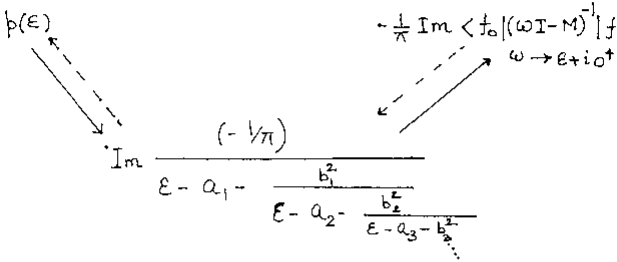

Fig. 2.1 Representation of three mathematical forms of positive, definite, integrable density function w finite moment.

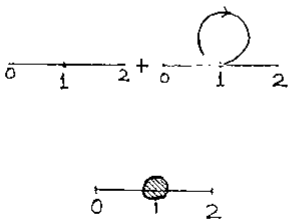

Fig. 2.2 Representation of a renormalised vertices.

continued fraction (i.e one has to follow the path shown in figure 2.1 by full lines) of the form as shown below :

$$p(\varepsilon+i\eta) = -\,\mathrm{Im}\lim_{\eta\to 0} \cfrac{(1/\pi)}{\varepsilon+i\eta - a_1 - \cfrac{b_1^2}{\varepsilon+i\eta - a_2 - b_2^2 \backslash}} \qquad (2.3)$$

such an expansion is convergent only if all the moments of $p(\varepsilon)$ are finite.

Having written the probability density in the above form the representation of the operator $M^{(1)}$ in some basis $|f_n\rangle$ can be written as a tridiagonal matrix with $a_1, a_2, a_3 \ldots$ etc along the diagonal and $b_1, b_2, b_3 \ldots$ etc along the off diagonal positions. It should be noted that for several distributions (like the Lorentzian), one cannot get a convergent continued fraction expansion. The whole thing breaks down as the moments of order > 2 are divergent.

Let us choose our system to be a random alloy A_cB_{1-c} having only the diagonal disorder and nearest neighbour overlap only. In the tight binding Anderson Hamiltonian

$$H = \sum \varepsilon_i P_i + \sum \sum V T_{ij} \qquad (2.4)$$

Here the diagonal terms ε_i form a set of random variables. In terms of the random *occupation* variables

$$\varepsilon_i = \varepsilon_A n_i + \varepsilon_B (1-n_i) \qquad (2.5)$$

The off diagonal term V , however, is not random.
$P_i = |i\rangle\langle i|$ is the Projection operator and $T_{ij} = |i\rangle\langle j|$ is the transfer operator in the space $\mathcal{H}$ spanned by the tight-binding basis $\{|i\rangle\}$.

Neglecting short range ordering, the probability density for the $\{n_i\}$ is given by

$$p(n_i) = c\,\delta(n_i-1) + (1-c)\,\delta(n_i)$$

$$= -(1/\pi)\ \mathrm{Im}\left[\frac{c}{n_i+i\eta-1} + \frac{(1-c)}{n_i+i\eta}\right] \qquad (\text{where } \eta \to 0^+)$$

$$= -(1/\pi)\ \mathrm{Im}\left[\frac{c}{N_i-1} + \frac{(1-c)}{N_i}\right] \quad (\text{Where } N_i = n_i+i\eta\ )$$

$$= -(1/\pi)\ \mathrm{Im}\ \frac{1}{N_i - c - \dfrac{c(1-c)}{N_i-(1-c)}}$$

$$= -(1/\pi)\ \mathrm{Im}\ \frac{1}{N_i - a_1 - b_1^2 / N_i - a_2} \qquad (2.6)$$

where $a_1 = c$; $a_2 = (1-c)$ and $b_1^2 = c(1-c)$

Thus $M^{(1)}$ has 2 × 2 tridiagonal matrix representation given by

$$\begin{pmatrix} c & \sqrt{c(1-c)} \\ \sqrt{c(1-c)} & 1-c \end{pmatrix} \qquad (2.7)$$

in a basis $\{|f_0^1\rangle, |f_1^1\rangle\}$ spanning the 'configuration space' ϕ_1 of n_1.

Let us consider the probability distribution for a single variable n_1 and the average of a function $F(n_1)$

$$\bar{F} = \int_{-\infty}^{\infty} F(n_1)\ p(n_1)\ dn_1$$

$$= -\int_{-\infty}^{\infty} F(N_1)\ (1/\pi)\ \mathrm{Im}\ g_{00}^{M}(N_1)\ dn_1 \qquad (2.8)$$

where, $N_1 = n_1 + i0^+$; $p(N_1) = -(1/\pi)\ \mathrm{Im} \langle f_0 | g^M(N_1) | f_0 \rangle$;
and $g^M(N_1) = (N_1 I - M^{(1)})^{-1}$

Let us consider F(z) as a function of a complex variable z having no singularities on the real axis in the neighbourhood of the branch cut of the function $g^{M}_{oo}(z)$. Then

$\bar{F} = -(1/2\pi i) \oint F(z)\, g^{M}_{oo}(z)\, dz$; where the contour is taken such that it goes round the branch cut of $g^{M}_{oo}(z)$.

$$= -(1/2\pi i) \oint F(z)\, dz \langle f_o | \int_{-\infty}^{\infty} (z-h)^{-1}\, dp(h) | f_o \rangle \qquad (2.9)$$

where $g^{M}(z) = \int_{-\infty}^{\infty} \frac{dp(h)}{z-h}$; and p(h) is spectral projection operator of $M^{(i)}$

Thus, $\bar{F} = \langle f^{1}_{o} | \int_{-\infty}^{\infty} F(h)\, dp(h) | f^{1}_{o} \rangle$

$$= \langle f^{1}_{o} |\, F(M^{(1)}) \,| f^{1}_{o} \rangle \qquad (2.10)$$

where the operator $F(M^{(i)})$ is the same functional of $M^{(i)}$ as F is of z. Thus we see that, in general, the configuration average can be written as a particular element of the representation of an operator constructed from the operator related to the probability distribution.

If we wish to generalise the theorem to functions of several independent random variables we introduce the

configuration space $\Phi = \Pi^{\otimes} \phi_i$ and $G(\{M^{(i)}\}) = \Pi^{\otimes} g^{M}(N_i)$. Then the average of the function $F(\{n_i\})$ is given by

$$\overline{F} = \int_{-\infty}^{\infty} \int_{-\infty}^{\infty} \{\Pi_i dn_i\} F(\{n_i\}) P(\{n_i\})$$

$$= \langle f_o | F(\{M^{(i)}\}) | f_o \rangle \qquad (2.11)$$

The configuration space $\Phi = \Pi^{\otimes} \phi_i$ is spanned by $\{|f_s\rangle = |f_{s_1}\rangle \otimes |f_{s_2}\rangle \otimes |f_{s_3}\rangle ..\}$ s is a composite index $\{s_1, s_2, s_3 \ldots s_N\}$ taking 2^N values, since each s_k can take values 0 and 1. $|f_o\rangle = |f_o^1\rangle \otimes |f_o^2\rangle \otimes |f_o^3\rangle \ldots |f_o^N\rangle$. $F(\{M^{(i)}\})$ is the same operator function of $\{M^{(i)}\}$ as $F(\{n_i\})$ was a function of $\{n_i\}$. This is the AUGMENTED SPACE THEOREM .

2.3 HAMILTONAN IN ASF FOR BOTH DIAGONAL AND OFF-DIAGONAL DISORDER

We will start with the tight binding multi-band Anderson Hamiltonian

$$H = \sum_i \sum_n \varepsilon_{in} |i,n\rangle\langle i,n| + \sum_{i \neq j} \sum_{n,m} V_{in,jm} |i,n\rangle\langle j,m| \qquad (2.12)$$

where, $\varepsilon_{in} = \varepsilon_{in}^{A} n_i + \varepsilon_{in}^{B} (1-n_i)$ (2.12a)

where i and j are the site indices and m,n are band indices.

$$V_{in,jm} = V_{nm}^{AA}\, n_i n_j + V_{nm}^{BB}\,(1-n_i)(1-n_j) + V_{nm}^{AB}\{\, n_i(1-n_j) + n_j(1-n_i)\} \qquad (2.12b)$$

Here, ε_{in} and $V_{in,jm}$ represent respectively diagonal and off-diagonal disorder arising from site energy and hopping integrals for the constituents A and B.

$$p(n_i) = c\,\delta(n_i-1) + (1-c)\,\delta(n_i) \qquad (2.13)$$

where, $n_i = 0, 1$

$$H = H_B + \sum_i \sum_n \varepsilon_n\, n_i P_{in} + \sum_{i\neq j} \sum_{n,m} V_{nm}^{(1)}\, n_i n_j\, T_{in,jm} + \sum_{i\neq j} \sum_{n,m} V_{nm}^{(2)}\,(n_i+n_j)\, T_{in,jm} \qquad (2.14)$$

where, $\varepsilon_n = (\varepsilon_A - \varepsilon_B)$; $V_{nm}^{(1)} = V_{nm}^{AA} + V_{nm}^{BB} - 2\,V_{nm}^{AB}$

and $V_{nm}^{(2)} = V_{nm}^{AB} - V_{nm}^{BB}$

The M^i for each value of n_i has a representation

$$\begin{bmatrix} c & \sqrt{c(1-c)} \\ \sqrt{c(1-c)} & 1-c \end{bmatrix} \qquad (2.15)$$

in the basis $|f_0^i\rangle$, $|f_1^i\rangle$ spanning ϕ_i.

The Augmented space Theorem then yields the Hamiltonian in the Augmented space as

$$\tilde{H} = H_B \otimes I + \sum_{i,n} \varepsilon_n P_{in} \otimes M^{(i)} \otimes I^{(i)}$$

$$+ \sum_{m,n} \sum_{i,j} V_{nm}^{(1)} T_{in,jm} \otimes M^{(i)} \otimes M^{(j)} \otimes I^{(ij)}$$

$$+ \sum_{n,m} V_{nm}^{(2)} \sum_{i \neq j} T_{in,jm} \otimes (M^{(i)} \otimes I^{(i)} + M^{(j)} \otimes I^{(j)}) \qquad (2.16)$$

$$\tilde{H} \in \mathcal{H} \otimes \prod_i^{\otimes} \phi_i$$

$I^{(i)}, I^{(ij)}$ in the above equation indicate identity operators in all subspaces ϕ_k except those superscripted.

2.4 CPA THROUGH THE AUGMENTED SPACE FORMALISM

Let us recapitulate the basic ideas behind single site CP approximation. We shall discuss the effective medium approach to derive the CPA equation. The tight binding Hamiltonian for a single band has the following form

$$H = \sum \varepsilon_i P_i + \sum V_{ij} T_{ij} \qquad (2.17a)$$

where ε_i takes the values ε_A or ε_B for binary alloy. ε_A and ε_B are site energies corresponding to A and B atoms respectively.

Thus,

$$[\ p^2/2m + V_i^c\ ]|i\rangle = \varepsilon_i|i\rangle \qquad (2.17b)$$

V_i^c = crystal potential corresponding to the i^{th} site.

$$V_{ij} = \langle i|\ \Sigma\ V_n^c\ |j\rangle \qquad (2.17c)$$

We now suppose that the Hamiltonian (2.17a) has only diagonal disorder i.e only ε_i is random. The underlying philosophy in a single site effective medium theory is that if any of the effective potentials $\Sigma(z)$ (coherent potential) are replaced by an exact potential ε_i there would be no extra scattering on the average. Mathematically it is equivalent to saying that average of the single site scattering t-matrix vanishes i.e

$$\tau_i(z) = \frac{(\varepsilon_i - \Sigma(z))}{\{1-(\varepsilon_i - \Sigma(z))\langle G(z)\rangle\}}$$

$$\langle \tau[\Sigma(z)] \rangle = 0 \qquad (2.18)$$

where,

$\Sigma(z)$ is the Coherent Potential. It is translationally symmetric, but a complex, energy dependent function.

$\langle G(z)\rangle$ is the configuration averaged diagonal element of the Green function for the alloy, which, by definition is the Green function for the Coherent potential

$$\langle G(z)\rangle = G_0(z-\Sigma(z)) \qquad (2.19)$$

Equation (2.18) together with Equation (2.19) constitute the self consistent equations in the single site CPA which has the following form :

$$\frac{c[\varepsilon_A-\Sigma(z)]}{1-[\varepsilon_A-\Sigma(z)]\,\langle G(z)\rangle} + \frac{(1-c)\,[\varepsilon_B-\Sigma(z)]}{1-[\varepsilon_B-\Sigma(z)]\,\langle G(z)\rangle} = 0 \qquad (2.20)$$

The above equation can be written in a more convenient form as follows:

$$\Sigma(z)= \bar{\varepsilon} + \frac{c(1-c)\langle G(z)\rangle(\varepsilon_A-\varepsilon_B)^2}{1-\{(1-2c)\delta + (\bar{\varepsilon}-\Sigma(z))\}\,\langle G(z)\rangle} \qquad (2.21)$$

where, $\bar{\varepsilon} = c\,\varepsilon_A+(1-c)\,\varepsilon_B$; $\delta =(\varepsilon_A-\varepsilon_B)$

We will now derive the same result via the Augmented Space formalism, in order to demonstrate the

equivalence of the two approaches.

We take a one atom cluster, i.e 0^{th} site as our 'cluster'.

By the Augmented Space theorem , we have

$$< G_{oo} > = <0,f_o| \ (zI-\tilde{H})^{-1}|0,f_o> \qquad (2.22)$$

Here $\tilde{H}$ is the expanded (Augmented space) Hamiltonian (2.16).

The configuration space for a single site is of rank 2, having $|f_o>$ and $|f_1>$ as the basis. The representation of $M^{(i)}$ is given by (2.15).

In operator form,

$$M^{(i)} = c|f_o^{(i)}><f_o^{(i)}| + (1-c)|f_1^{(i)}><f_1^{(i)}|$$

$$+ \sqrt{c(1-c)} \ (|f_o^{(i)}><f_1^{(i)}| + |f_1^{(i)}><f_o^{(i)}| \ )$$

We now partition the expanded Hamiltonian $\tilde{H}$ into the space I spanned by $|0f_o>$ and $|0f_1>$ and space II by the rest of the medium which we will replace by the effective medium. We will need to evaluate the elements of $\tilde{H}$ in the space I only.

We have,

$$H_e = \Sigma \ \epsilon_o P_o + \Sigma \ V_{ij} \ T_{ij}$$

$$= \varepsilon_B + \delta\varepsilon \sum_i n_i P_i + \sum_{i,j} V_{ij} T_{ij} \qquad (2.23)$$

where, $\delta\varepsilon = \varepsilon_A - \varepsilon_B$

$$\tilde{H} = H_e + (-\Sigma_0 + \tilde{\varepsilon}) P_0 \qquad (2.24)$$

where, $\tilde{\varepsilon} = (1-c)\varepsilon_A + c\,\varepsilon_B$

We shall first evaluate the matrix elements of $\tilde{H}$ in the space I

$$\langle 0,f_0|\tilde{H}|0,f_0\rangle = \varepsilon_B + \delta\varepsilon \sum_i \langle 0,f_0|\left\{|i\rangle\langle i|\otimes M^{(i)}\right\}|0,f_0\rangle$$

$$+\sum_{i,j} V_{ij} \langle 0,f_0|\left\{|i\rangle\langle j|\otimes I\right\}|0,f_0\rangle$$

$$= \varepsilon_B + \delta\varepsilon \sum \delta_{i0} \langle f|M^{(i)}|f\rangle$$

$$+ \sum_{i,j} V_{ij}\delta_{i0}\delta_{j0}\langle f|f\rangle \quad ; \ \delta_{i0}\,\delta_{j0} = 0 \ , \text{ for } i\neq j$$

$$= \varepsilon_B + \delta\varepsilon \langle f|M^{(i)}|f\rangle$$

$$= \varepsilon_B + \delta\varepsilon\, c = \bar{\varepsilon} \quad ; \quad \text{where } \bar{\varepsilon} = c\varepsilon_A + (1-c)\varepsilon_B$$

Thus, $\langle 0,f_0|\tilde{H}|0,f_0\rangle = \bar{\varepsilon}$ (2.25a)

$$\langle 0,f_1|\tilde{H}|0,f_1\rangle = \varepsilon_B + \delta\varepsilon \sum_i \langle 0,f_1|\left\{|i\rangle\langle i|\otimes M^{(i)}\right\}|0,f_1\rangle$$

$$+ \sum_{i,j} V_{ij} \langle 0,f_1|\left\{|i\rangle\langle j|\otimes I\right\}|0,f_1\rangle$$

$$= \varepsilon_B + \delta\varepsilon \sum_i \delta_{i0} \langle f_i | M^{(i)} | f_i \rangle$$

$$+ \sum_{i,j} V_{ij} \delta_{i0} \delta_{j0} \langle f_i | f_i \rangle$$

$$= \varepsilon_B + \delta\varepsilon \ (1-c) = \tilde{\varepsilon} \qquad (2.25b)$$

$$\langle 0, f_0 | \tilde{H} | 0, f_i \rangle = \varepsilon_B \langle f_0 | f_i \rangle + \delta\varepsilon \sum_i \langle 0, f_0 | \left\{ |i\rangle\langle i| \otimes M^{(i)} \right\} | 0, f_i \rangle$$

$$+ \sum_{i,j} V_{ij} \langle 0, f_0 | \left\{ |i\rangle\langle j| \otimes I \right\} | 0 f_i \rangle$$

$$= \delta\varepsilon \sum_i \delta_{i0} \langle f_0 | M^{(i)} | f_i \rangle + \sum_{i,j} V_{ij} \delta_{i0} \delta_{j0} \langle f_0 | f_i \rangle$$

$$= \delta\varepsilon \langle f_0 | M^{(0)} | f_i \rangle = \delta\varepsilon \sqrt{c(1-c)} = W \qquad (2.25c)$$

Similarly, one can show $\langle 0 f_i | \tilde{H} | 0 f_0 \rangle = W$ (2.25d)

Now, $[zI - H]^{-1} = [zI - \{ H_e + (-\Sigma_0 + \tilde{\varepsilon}) P_0 \}]^{-1}$

$$= [(zI - H_e) - (\tilde{\varepsilon} - \Sigma_0) P_0]^{-1}$$

$$= [\langle G \rangle^{-1} - (\tilde{\varepsilon} - \Sigma_0) P_0]^{-1}$$

$$= [I - (\tilde{\varepsilon} - \Sigma_0) \langle G \rangle P_0]^{-1} \langle G \rangle$$

$$\text{So, } G^{(of_0)}_{of_i, of_i} = \frac{\langle G_{00} \rangle}{1 - (\varepsilon - \Sigma_0) \langle G_{00} \rangle} \qquad (2.26)$$

Thus, we have

$$\Sigma_o = \bar{\varepsilon} + W\, G_{of_1, of_1}^{of_o} W$$

$$= \bar{\varepsilon} + \frac{c(1-c)\,(\varepsilon_A - \varepsilon_B)^2 \langle G_{oo} \rangle}{1-(\varepsilon - \Sigma_o)\langle G_{oo} \rangle} \qquad (2.27)$$

The above equation (2.27) is identical to the equation (2.21) when we substitute the value of $\tilde{\varepsilon}$. Thus we have been able to show that CPA results can be derived via the ASF.

2.5 CLUSTER COHERENT POTENTIAL APPROXIMATION (CCPA) IN THE AUGMENTED SPACE BY GRAPHICAL METHODS

We start from the configuration averaged Green function

$$\langle G_{in,jm}(z) \rangle = \langle r_i \; n \; f_o | (z\tilde{I} - \tilde{H})^{-1} | r_j \; m \; f_o \rangle \qquad (2.28)$$

where $|f_o\rangle = \prod_i \otimes |f_o^i\rangle$

At this stage we shall digress to discuss a graphical method for the calculation of Green functions and related resolvents. The method was discussed in this connection first by Haydock (1972). It is an attractive

alternative to the algebraic multiple scattering methods in that it clearly, visually illustrates some of the cumbersome algebraic expressions

2.51 THE GRAPHICAL METHOD

By a graph we mean a set of *vertices* connected by *links*. Let $\{|\nu\rangle\}$ be any complete linearly independent basis in which the Hamiltonian is described. The overlap matrix $S_{ij} = \langle i|j\rangle$ is a unit matrix provided the basis is orthonormal. Matrix elemments of an operator **M** are given by $M_{ij} = \langle i|M|j\rangle$. A graph is associated with every basis $\{|\nu\rangle\}$. To every element $|\nu\rangle$ of the basis set $\{|\nu\rangle\}$ is associated a vertex V_i and to each distinct pair of elements $(|\nu\rangle,|\mu\rangle)$ a *link* or *bond* l_{ij} which may be directional (i.e l_{ij} may not be be equal to l_{ji}) or otherwise. To any operator **M** there corresponds a graph consisting of vertices and links for which $M_{ij} \neq 0$. If we want to invert an operator **M** then the *contribution* of each vertex V_i is defined as

$$K(V_i) = 1/M_{ij}$$

and that of the link l_{ij} as

$$K(l_{ij}) = M_{ij}$$

A path of length n is a sequence of vertices connected by n links

$$\mathcal{P}_n = \{V_i l_{ij} V_j l_{jk} \ldots \}$$

Contribution of a path of length n is given by

$$K(\mathcal{P}_n) = \prod_{i=1}^{n+1} K(V_i) \prod K(l_{ij}) \qquad (2.28)$$

The Green function $G_{ij}(z) = \sum_{n=0}^{\infty} \sum_{\mathcal{P}_n \in \delta_n} K(\mathcal{P}_n)$, where δ_n is the set of all paths connecting the vertices V_i and V_j.

It is well known that the enumeration or even statistical estimation of all paths between two vertices on a general lattice is not a tractable problem. We therefore go through a renormalisation procedure.

Let us introduce the definition of a *non-intersecting* path $\mathcal{P}_n'$. A path $\mathcal{P}_n' = \{V_0 l_{01} V_1 l_{12} \ldots V_n\}$ is *non-intersecting* if none of the internal vertices $V_1 \ldots V_{n-1}$ are the same. If $V_0 = V_n$ then the path is a *closed, or polygonal* non-intersecting path.

We now gather together all paths starting from V_0, going through V_1 to V_2 either directly or via other vertices.

This renormalises the vertices V_i (see figure (2.2)). If we do this for every vertex, we obtain at the end only non-intersecting paths but the contribution $K(V_n)$ is renormalised to

$$K'(V_n) = G_{nn}^{(0,1,\ldots n-1)}(z) \qquad \text{(Haydock 1972; Mookerjee 1979)} \tag{2.30}$$

the superscripts denote that the Green function is calculated on a graph in which the superscripted vertices are absent and

$$G_{ij}(z) = \sum_{n=0}^{\infty} \sum_{\mathcal{P}_n \in \delta'_n} K'(\mathcal{P}_n) \tag{2.31}$$

where δ'_n are the set of non-intersecting path of length n from V_i to V_j on the lattice. The expression is identical to Feenberg renormalised perturbation expansion.

On the Augmented Space each vertex is specified by two indices : one referring to the site on the lattice and the other the configuration.

Configurations may be conveniently labelled as follows:

$$|f_o\rangle = \Pi^{\otimes} |f_o^{(i)}\rangle$$

$$|f_{jk\ldots}\rangle = \Pi^{\otimes}_{i \neq j,k} |f_o^{(i)}\rangle \; \Pi^{\otimes}_{m=j,k} |f_1^{(m)}\rangle$$

2.52 THE CPA IN THE GRAPHICAL METHOD

The CPA retains contributions of all paths between vertices having the same configuration and different sites or the same site and configuration that differ *only* at that site e.g $|s,f_{jk}\rangle$ and $|s,f_{jks}\rangle$.

The Augmented space ($\Psi = \mathscr{H} \otimes \Phi$)Hamiltonian in the site-configuration representation $|nf\rangle$ is given by

$$\tilde{H}_{nf,mf'} = M^{n}_{ff'}\delta_{nm} + V_{nm}\delta_{ff'} \qquad (2.32)$$

where, $M^{n}_{ff'}$ is an operator in the configuration space associated with the probability distribution and V_{nm} is an operator in $\mathscr{H}$. The states in the configuration space are specified by the set $\{|f^{n}_{i}\rangle\}$. In general, we choose a basis such that the representation of M^{n} is tridiagonal so that $p(\varepsilon)$ is expressed as a continued fraction. For a bimodal density the $M^{n}_{ff'}$ for each n is given by equation (2.15) and its graph is a single link chain like (Fig 2.3a). Finally the configuration averaged Green function is the resolvent corresponding to the Hamiltonian $\tilde{H}$.

The configurationally averaged Green function $\langle G_{nm}(z)\rangle$ can be determined by considering self avoiding paths between $|nf_{o}\rangle$ and $|mf_{o}\rangle$ in the complete Augmented space Ψ .In

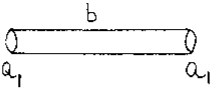

Fig. 2.3a Representation of a single link chain

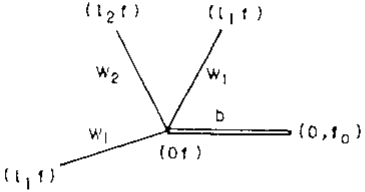

Fig.2.3b CPA graph in Augmented space

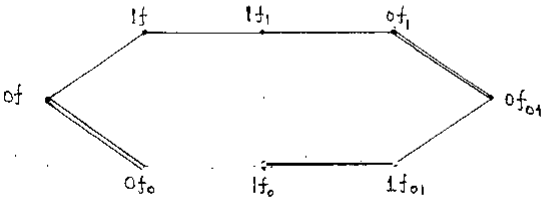

Fig. 2.3c Shortest self avoiding,closed loop in the full Augmented space involving both spatial and field hops.

Ψ, an electron at site labelled by n and configuration state $|f_{i,\ldots k}\rangle = |f_i^1\rangle \otimes |f_j^2 \otimes \ldots |f_k^n\rangle$ can either make spatial hops to one of the near neighbours of n with matrix element V, keeping the configuration state the same, or it can remain on the spatial site, while the configuration only at that site changes while those at all other sites remain the same. This hop is with matrix element M.

$$\langle G_{nm}(z)\rangle = \langle n\ f_o|\ (zI - \tilde{H}\ )^{-1}|m\ f_o\rangle \qquad (2.33)$$

here, the problem is reduced to that of an ordered system with a much amplified set of eigen functions.

Now starting from the vertex (0f) the first steps in the self-avoiding paths possible are the near neighbours 1_i in the real space shown by the single lines in figure (2.3b) or to different configuration states of the site 0 (For example the one labelled by $0f_o$) shown by double lines in the same figure.

If $R_o(z)$ is the contribution of all self avoiding paths from vertex 0 and back in the Hilbert space $\mathcal{H}$, then the resolvent in an ordered system is

$$P_{oo}(z) = \frac{1}{z - R_o(z)} \qquad (2.34)$$

In the three dimensional case $R_o(z)$ will include the contribution $\sum_i V_i^2 P_{oo}^{(i)}$ [where i are the various neighbours of O and $P_{ii}^{(i)}$ is the resolvent calculated from a sub graph in which the vertex O is removed], as well as the contributions of closed self avoiding loops in $\mathcal{R}$. In the extended space, the configuration averaged Green function is given by

$$\langle G(z) \rangle = \frac{1}{z - R(z) - T(z)} \qquad (2.35)$$

R(z) is the contribution of non intersecting paths from the vertex Of and back that are either (a) entirely in the spatial part of the Augmented space which is same ones as those that contribute to R(z), or (b) self avoiding paths in the Augmented space which includes field-hops but do not form closed loops. T(z) is the contribution of the closed non intersecting loops from Of in the full Augmented space.

Figure (2.3c) shows a self avoiding closed loop involving both spatial and field hops. There are numerous loops like this and it is almost impossible to account for all of them. So as an approximation we assume that all closed

paths having both spatial and field hops be delinked i.e T(z)=0. Once we have done that,our approximate graph will have the following topology : (a) from every spatial site there is now an extra field hop with link function W. Every vertex looks like figure (2.3b);and (b) if starting from a vertex'nf_s' we hop to a vertex 'nf_n'then the subgraph with vertex 'nf' missing is an infinite graph exactly similar to the original one. A direct consequence of this property is

$$G^{(of)}_{of_o,of_o} = G_{of,of} = \langle G_{oo} \rangle \qquad (2.36)$$

This will not hold in the absence of delinking as above.

Let $G^{DL}(z)$be the resolvent,corresponding to the delinked graph in the Augmented space and let

$$M_{ij} = W_i \delta_{j,i+1}$$

be the tridiagonal representation of the operator M^n in the each subspace $|f^{(i)}_o\rangle$ of $|f_o\rangle$. Then

$$G^{DL}(z) = \frac{1}{[\, z - R_o(z - W^2 G_1(z)) - W^2 G_1(z)]}$$

$$= P_{oo}[\, z - W_1^2\, G_1(z)] \qquad (2.37)$$

where, $G_{ii}(z) = \dfrac{1}{z - R_0(z-W_i^2 G_i)-W_{i+1}^2 G_{i+1}(z)}$ (2.38)

In the conventional CPA formalism, the self energy $\Sigma(z)$ is expressed as

$$G^{CP}(z) = \frac{1}{z - \Sigma(z) - R_0(z-\Sigma)}$$

$$= P_0 [z - \Sigma(z)] \qquad (2.39)$$

Equations(2.39) and (2.37) show the equivalence. Equivalence of the two has been discussed in detail by Bishop and Mookerjee (1974).

2.6 THE CLUSTER GENERALISATION : THE SELF CONSISTENT EFFECTIVE MEDIUM IN AUGMENTED SPACE

The generalisation to a CCPA with a cluster given by the sites (s,t,...v) retains contribution of all paths between vertices having the same configuration and different sites or between the same site s, and configurations which differ only at those sites which belong to the same cluster as s, e.g $|s,f_{jk}\rangle$, $|s,f_{jks}\rangle$, $|s,f_{jkt}\rangle$....$|s,f_{jkv}\rangle$

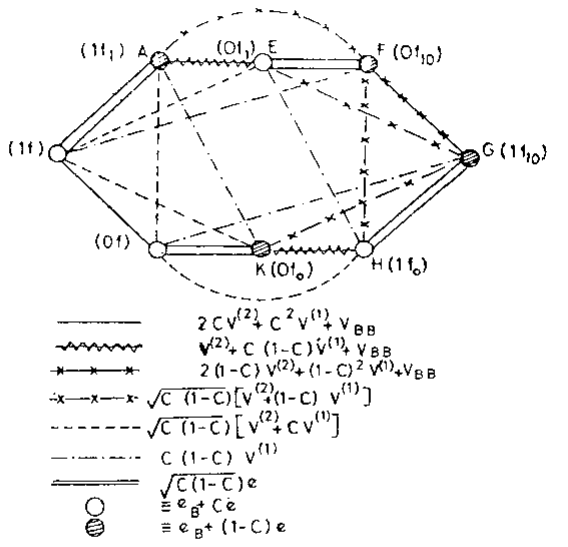

Fig. 2.4a Octagonal decoration corresponding to 2CPA in Augmented space.

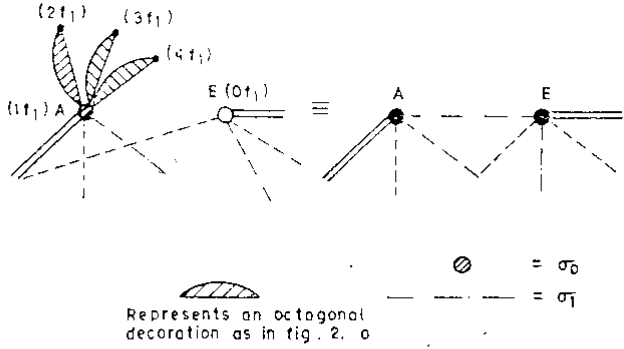

Fig. 2.4b Renormalisation of site and bond of the octagon in ASF due to infinite medium.

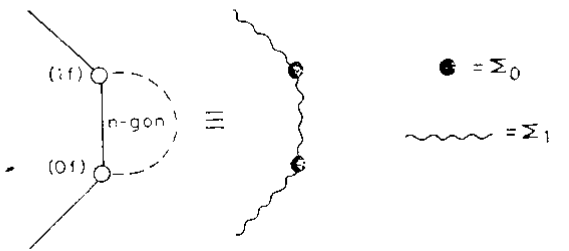

Fig. 2.4c Final renormalised site and bond in 2CPA for the octagon in Fig. 2.4a

The polygonal self avoiding paths which take into account the multiple scattering within the cluster are immersed in the rest of the lattice and consequently the vertices and links (bonds) have to be renormalised accordingly. We will as an example see how this is done for the 2CPA for a binary alloy. Corresponding to the 2-site cluster, we have an octagonal decoration of self avoiding polygonal paths in the Augmented Space graph shown in the figure (2.4a).The eight vertices of the octagon correspond to the eight different configurations of the two site cluster (2×2^2). The octagon belonging to a bond has no connection to another bond through links in the Augmented Space, which effectively ensures that the correlated scattering from three or more sites belonging to different bond is ignored.

Finally, we renormalize the vertices and bonds in the following way. The renormalisation is a two step process.

STEP 1

The decorating octagon is not an isolated octagon involving only the two spatial sites(0 and 1). If we consider the vertex A ($1f_1$ in the notation of Mookerjee(1973)) the bond AE ($1f_1$ to $0f_1$) belonging to the octagon is only one of the Z nearest neighbours of 1. The other remaining (Z-1) bonds viz $1f_1$to $2f_1$,$3f_1$,....etc. also hang on to site A. Besides, these bonds themselves in turn have their octagons

decorating them (Fig 2.4b). Thus the bond AE is itself immersed in a self-consistent medium. The same is true for the bonds FG, and HK of the octagon. We may take this into account by saying that the medium renormalises the bonds AE, FG and HK and the sites at their extremities. Once this normalisation is carried out, the octagon is effectively isolated. The renormalised vertices $\sigma_0(z)$ and bonds $\sigma_1(z)$ are found as below:

We divide the whole lattice into two subspaces labelled by (1) and (2). (1) is a unrenormalized bond AE with a Hamiltonian

$$H^{(1)} = V_2 \ (\ T_{AE} + T_{EA} \ ) \qquad (2.40)$$

and (2) a lattice $\mathcal{L}$ which is the original lattice minus the link AE and in which all bonds and sites are renormalised.

This has a Hamiltonian

$$H^{(2)} = \Sigma_0(z) \sum_{i \neq A,E} P_i + \Sigma_1(z) \sum_{i,j \neq A,E} T_{ij} \qquad (2.41)$$

also there is a linking Hamiltonian between (1) and (2).

$$H^{(int)} = \Sigma_1(z) \sum (T_{iA} + T_{Ai} + T_{iE} + T_{Ei}) \qquad (2.42)$$

Now Green's operator corresponding to the subspace (1),

$$G^{(1)} = P_1 G P_1 = \left(zI - H^{(1)} - H^{(1,2)} G^{(2)} H^{(2,1)} \right)^{-P_1} \qquad (2.43)$$

where, X^{-P_Y} is the invrese of the operator X in the subspace Y.

G is Green's operator in the total space and $G^{(2)}$ is $(zI - H^{(2)})^{-P_2}$ with

$$P_1 + P_2 = I \qquad (2.44)$$

It is obvious from above equation that the effect of the rest of the lattice hanging on to the bond AE is to change the Hamiltonian $H^{(1)}$ to $H^{(1)}+\sigma$ where the self energy σ is given by

$$\begin{aligned} \sigma_{AA} = \sigma_{EE} = \sigma_0(z) &= \Sigma_1^2(z) \sum_{k,m \in N_A} G^{(z)}_{km} \\ \sigma_{AE} = \sigma_{EA} = \sigma_1(z) &= \Sigma_1^2(z) \sum_{k \in N_A} \sum_{m \in N_E} G^{(2)}_{km} \end{aligned} \qquad (2.45)$$

where, N_A are the nearest neighbour of A ; N_E are the nearest neighbour of E.

STEP 2

We are now left with the isolated renormalised

octagon. This octagon is to be renormalised again because each of the vertices such as A,E etc are connected with other vertices through either a field hop or spatial hop. For carrying out this final renormalisation we divide the octagon into two subsystems : bond B (0f,1f) and the rest of the octagon M.

$$\tilde{H}^{B} = \sum_{i}\sum_{j\in 0f,1f} \tilde{H}_{ij} \; ; \; \tilde{H}^{M} = \sum_{i}\sum_{j\in 0f,1f} \tilde{H}_{ij} \qquad (2.46)$$

$$\tilde{H}^{BM} = \sum_{i\in B}\sum_{j\in M} (\tilde{H}_{ij} + \tilde{H}_{ji}) \qquad (2.47)$$

Now,we have as before,

$$G^{B} = P_{B} G P_{B}$$

$$= [zI - \tilde{H}^{B} - \tilde{H}^{BM} G^{M} \tilde{H}^{BM}]^{-P_{B}} \qquad (2.48a)$$

and $$G^{M} = [zI - \tilde{H}^{M}]^{-P_{M}} \qquad (2.48b)$$

Now we have the final renormalised site $\Sigma_{0}(Z)$ and bond $\Sigma_{1}(z)$ given by :

$$\Sigma_{0}(z) = \tilde{H}^{B}_{00} + \sum_{j\neq 0}\sum_{k\neq 1} \tilde{H}^{BM}_{0j} G^{M}_{jk} \tilde{H}^{BM}_{k0}$$

$$\Sigma_{1}(z) = \tilde{H}_{01} + \sum_{j\neq 0}\sum_{k\neq 1} \tilde{H}^{BM}_{0j} G^{M}_{jk} \tilde{H}^{BM}_{k1} \qquad (2.49)$$

Equations (2.45) and (2.49) are the set of self consistent form of Equations which provides self consistent effective medium.

$$\Sigma = \begin{bmatrix} \Sigma_o & \Sigma_1 \\ \Sigma_1 & \Sigma_o \end{bmatrix} \qquad (2.50)$$

The Green function may now be calculated

$$H_{eff} = \sum \Sigma_o P_i + \sum \Sigma_1 T_{ij}$$

$$= \Sigma_o I + (\Sigma_1 / V) \sum_{ij} V T_{ij}$$

$$= \Sigma_o I + (\Sigma_1 / V) h_o \qquad (2.51)$$

Where $h_o = \sum V T_{ij}$

$$\langle G(z) \rangle = (zI - H_{eff})^{-1}$$

$$= [(z-\Sigma_o) I - (\Sigma_1 / V) h_o]^{-1}$$

$$= (V/\Sigma_1)[((Z-\Sigma_o)V/\Sigma_1) I - h_o]^{-1}$$

$$= (V/\Sigma_1) G(\xi) \qquad (2.52)$$

where, $\xi = (z-\Sigma_o)V/\Sigma_1$ and $G(z) = (zI - h_o)^{-1}$

Once we calculate G(z) by methods available for translationally symmetric Hamiltonians, the equations (2.45) to (2.52) are the basic equations governing the CCPA.

CHAPTER III

RECURSIVE SOLUTION TO THE SCHRODINGER EQUATION

3.1 THE RECURSION METHOD

In simple metals, where the effective, screened interaction between electrons and atoms is not so strong, the electronic structure is determined by the long range periodicity of the atomic potentials. It is this aspect of physics that is exploited in the band theory to express electronic properties of the solid as a coherent superposition of the electronic properties of the atoms. However, when the electrons interact strongly with the atoms, this picture breaks down and properties no longer depend on long range periodicity, but rather on only the first few shells of neighbours of each atom. The d-electrons in transition metals are typical examples of this regime. While the band theory is still a valid formal solution to the Schrödinger equation, the physics is better understood by means of a solution that explicitly accounts for the role of the local environment.

The basic problem is to find the local density of states from a tight binding or localised orbital model. The underlying physics in the recursion method (Haydock 1980) is that the local orbital itself has the greatest effect on the local electronic structure and successively more distant orbitals have lesser effect. The solution must define a hierarchy of environments so that their relative influence is explicitly displayed in the local density of states. Phyaically, the local denaity of states is the intensity of each eigenstate on a particular atom or bond. Mathematically, it is the squared magnitude of the projection of an eigen state on a local orbital, so that the local density of states gives the coupling of an orbital at each energy.

The problem is the determination of linear combinations of the local orbitals such that the electron must pass through each state as it diffuses away from the local orbital from which it starts. The local density of states for a basis orbital $|\phi_o\rangle$ is determined by the sequence of environments described by orthogonal states $|U_n\rangle$, where $|U_n\rangle$ is a linear combination of basis orbitals and $|U_o\rangle$ is $|\phi_o\rangle$. $|U_n\rangle$ must satisfy the condition that

$$H|U_n\rangle = a_n|U_n\rangle + b_{n+1}|U_{n+1}\rangle + b_n|U_{n-1}\rangle \qquad (3.1)$$

where H is the Hamiltonian of the model and $|U_n\rangle$ are

localised on the shell of atoms n hops from the atom accommodating $|\phi_o\rangle$. The parameters a_n and b_n describe the coupling of each environment to itself and its neighbours. The purpose of going over to such a basis set is that one can transform any three dimensional model to a pseudo one-dimensional equivalent chain, which is characterised by the parameters a_n and b_n the coupling constants of each environment to itself and its neighbours.

The coefficients a_n and b_n are generated recursively from

$$|U_o\rangle = |\phi_o\rangle \ , \ b_o = 1$$

$$a_n = \frac{\langle U_n|H|U_n\rangle}{\langle U_n|U_n\rangle}$$

$$b_{n+1} = \frac{b_n \langle U_n|U_n\rangle}{\langle U_{n+1}|U_{n+1}\rangle} \qquad (3.2)$$

We have used the orthogonality of the new basis $\{U_n\}$. The above equations are a convenient algorithm for computational generation of the coefficients a_n and b_n.

As an example, the local density of states for $|\phi_o\rangle$ can be written in terms of the parameters of the chain model

Let us define the determinant of the matrix with the first n rows and n columns deleted as $D_n(E)$

$$G_0(E) = \frac{D_1(E)}{D_0(E)}$$

$$= \frac{D_1(E)}{(E - a_0)\, D_1(E) - b_1^2\, D_2(E)}$$

$$= \frac{1}{(E-a_0) - b_1^2\, D_2(E)/D_1(E)}$$

$$= \frac{1}{(E-a_0) - b_1^2\, G_1(E)}$$

as the continued fraction

$$n_o(E) = -(1/\pi)\ \mathrm{Im}\ \{\ 1/\!\!-\ (E-a_o-b_1^2/\!\!-\ (E-a_1-b_2^2/\!\!-\ (E-a_2-b_3^2/\!\!-\ .)$$

where, $H_{n,n} = a_n$; $H_{n,n+1} = H^*_{n+1,n} = b_n$ (3.3)

Let us try to get the continued fraction for local density of states $n_o(E)$ starting from the Green function. One can immediately check that in the above basis set $|U_n\rangle$ the Hamiltonian is a tridiagonal matrix

$$\begin{bmatrix} a_o & b_1 & 0 & 0 & \cdots \\ b_1 & a_1 & b_2 & 0 & \cdots \\ 0 & 0 & b_2 & a_2 & \cdots \\ 0 & 0 & b_3 & a_3 & \cdots \\ \cdot & \cdot & \cdot & \cdot & \cdots \end{bmatrix}$$

$$G_o(E) = \langle \Psi_o | (zI-H)^{-1} | \Psi_o \rangle$$

$$= \begin{bmatrix} (E-a_o) & -b_1 & 0 & 0 & \cdots \\ -b_1 & (E-a_1) & -b_1 & 0 & \cdots \\ 0 & -b_2 & (E-a_2) & -b_3 & \cdots \\ 0 & 0 & -b_3 & (E-a_3) & \cdots \\ \cdot & \cdot & \cdot & \cdot & \end{bmatrix}^{-1}$$

Let us define the determinant of the matrix with the first n rows and n columns deleted as $D_n(E)$

$$G_0(E) = \frac{D_1(E)}{D_0(E)}$$

$$= \frac{D_1(E)}{(E - a_0)\, D_1(E) - b_1^2\, D_2(E)}$$

$$= \frac{1}{(E-a_0) - b_1^2\, D_2(E)/D_1(E)}$$

$$= \frac{1}{(E-a_0) - b_1^2\, G_1(E)}$$

If we continue this process upto n-steps, we have

$$G_0(E) = \frac{1}{E-a_0 - b_1^2 / (E-a_1 - b_2^2 / \ldots\ldots (E-a_{n-1} - b_n^2\, G_n(E))} \qquad (3.4)$$

where,

$$G_n(E) = \frac{1}{E-a_n - b_{n+1}^2\, G_n(E)}$$

Thus $G_0(E)$ has a continued fraction representation

which in general may not terminate after a finite number of steps. It has been verified that for many systems the continued fraction converges very fast. When the convergence is slow or oscillatory it can be terminated by various termination schemes. Several termination schemes have been developed by Nex (1978,1984) and Haydock and Nex (1984).

3.2 THEORY OF CONTINUED FRACTION TERMINATORS

For applying the termination scheme to approximate the tail of the continued fraction for the Green function, we have to ensure that the approximate resolvent R(z) (which replaces G) should be such that the corresponding Hamiltonian H should have a similar energy spectrum. By a similar energy spectrum we mean that it should possess as many singularities as the spectrum of the true Hamiltonian i.e band-edges, van Hove singularities and so on.

The continued fraction form of the Green function for a uniform chain parameter i.e $a_n = a$, $b_n = b$ is

$$G_o(E) = \frac{1}{E-a-b^2 G_o(E)}$$

or, $b^2 G_o^2(E) - (E-a)G_o(E) + 1 = 0$

Therefore,

$$G_o(E) = \frac{(E-a_o) \pm \sqrt{(E-a)^2 - 4b^2}}{2b^2} \qquad (3.5)$$

Here we need not use the termination scheme because the Green function is exact. The negative sign is chosen in (3.5) to ensure a Herglotz $G_o(E)$. The Green function has two band edge singularities at $E_1 = a + 2b$ and $E_2 = a - 2b$ and a branch cut between these energies along the real energy axis.

Let us now consider a general system having a single band Hamiltonian. In this case, the square root terminator (3.5) is appropriate as shown by Haydock and Nex (1984). We illustrate mathematically below. We have the Green function

$$G(E) = \cfrac{1}{E-a_0 - \cfrac{b_1^2}{E-a_1 - \cfrac{b_2^2}{\ddots - \cfrac{b_{n-2}^2}{E-a_{n-2} - \cfrac{b_{n-1}^2}{E-a_{n-1} - t(E)}}}}} \qquad .....(3.6)$$

where t(E) is the required terminator

Since the eigenstate of the chain is some linear combination of the states $|U_0\rangle$, $|U_1\rangle$....we write the

Schrödinger equation for the chain in the following form

$$H \sum_{n}^{\infty} p_n U_n = E \sum_{n}^{\infty} p_n U_n \qquad (3.7a)$$

In matrix form:

$$\begin{bmatrix} (E-a_0) & -b_1 & 0 & \cdots \\ -b_1 & (E-a_1) & -b_1 & \cdots \\ 0 & -b_2 & \cdot & \cdots \\ \cdot & \cdot & \cdot & \cdots \\ \cdot & \cdot & \cdot & \cdots \\ \cdot & \cdot & \cdot & \cdots \end{bmatrix} \begin{bmatrix} p_0 \\ p_1 \\ p_2 \\ \cdot \\ \cdot \\ \cdot \end{bmatrix} = 0 \qquad (3.7b)$$

The recursion coefficients can be found in terms of orthogonal polynomials. We use those of the first kind $P_i(E)$ and second kind $q_i(E)$. Now making a proper choice of boundary conditions such that

$$P_{-1} = 0 = q_{-1} \quad ; \quad P_0 = 1 \; ; \quad q_0 = b_0^2 \qquad (3.8a)$$

We have,

$$P_{i+1}(E) = (E-a_i)\, P_i(E) - b_i^2\, P_{i-1}(E)$$

$$q_i(E) = (E-a_i) q_{i-1}(E) - b_i^2\, q_{i-2}(E) \qquad (3.8b)$$

We may write

$$G(E) = \frac{q_{n-2}(E) - b^2_{n-1} t(E)\, q_{n-3}(E)}{p_{n-1}(E) - b^2_{n-1} t(E)\, p_{n-2}(E)} \qquad (3.9)$$

3.21 TERMINATER SCHEMES

We have three termination techniques, of which two are explicit and require further physical input in the form of analytic properties of the Green function , while in the third case no further assumptions are required and is implicit in terms of the terminator function t(E) in equation (3.6). Haydock (1980) and Haydock and Nex (1984),have provided two explicit termination techniques based on generating an analytic form for t(E) for the single band density of states and for many band case respectively. The third method is an implementation of the quadrature approach.

For the case of single band density of states, the square root terminator is appropriate and we have

$$t(E) = \frac{[\ E - (\alpha+\beta)/2 - \sqrt{(E-\alpha)(E-\beta)}\ ]}{2b^2} \qquad (3.10)$$

where $E = \alpha$ and $E = \beta$ correspond to the band edges and $b = (\beta-\alpha)/4$. In the multiband case, we use a model Greenian F(E) [Haydock and Nex(1984)], with square root band-edge singularities,

$$F(E) = \sum_j 8N_j[\ E-(\alpha_j+r_j/2)- \sqrt{(E-\alpha_j)(E-\alpha_j-r_j)}\ ]/\ r_j^2 \qquad (3.11)$$

Here α_j's, r_j's and N_j's are respectively the left band edges, the band widths and the band weights (the number of states in the j^{th} band) as j runs over all the bands. The continued fraction corresponding to F(E) is generated using the recursion algorithm with H replaced by E, vectors by polynomials and the vector inner product by that generated by F. Based on classical generation of orthogonal polynomials (Cheney, 1966), Haydock and Nex (1984) described the inner product for this particular Greenian as a union of Gauss-Chebyshev quadratures:

$$\langle f,g \rangle = \sum_{i=1}^{n} \sum_j \omega_{ij}\ f(x_{ij})\ g(x_{ij}) \qquad (3.12)$$

where, $\omega_{ij} = \pi N_j / (n+1) \sin^2\theta$; $x_{ij} = \alpha_j + (1-\cos\theta_j) r_j/2$

and $\theta = i\pi / (n+1)$

This provides the general form of terminator for most three-dimensional model calculations. In case other analytic forms F(E) are required one can use the supplied basic routines to generate the corresponding three term recurrence explicitly or through the use of an appropriate numerical quadrature rule. Let $r_i(E)$ and $s_i(E)$ be the orthogonal polynomials corresponding to F(E) just as we have p_i and q_i for G(E) before, then the terminator is given by

$$t(E) = \frac{s_{n-2}(E) - F(E)\, r_{n-1}(E)}{d^2_{n-1}[\, s_{n-3}(E) - F(E) r_{n-2}(E)]} \qquad (3.13)$$

The third termination scheme, the quadrature approach does not generate t(E) explicitly, but in some sense averages over all possible values of t(E). In this case, the integral density of states

$N(E) = \int_0^E n(x)dx$ is approximated by $\sum_{E_i < E} \omega(E_i(E)) + \alpha\, \omega(E)$ (3.14)

where α is a constant which usually takes the values 0.5 and E_i's are the Eigen values of the Jacobi matrix (3.2)

extended by generating a new coefficient

$$a_{n-1} = E - b^2_{n-1} p_{n-2}(E) \;/\; p_{n-1}(E) \qquad (3.15)$$

This ensures that at least one of the E_i say E_m is equal to E.

Then the density of states is approximated by

$$n(E) = \frac{p'_n(E)}{p_{n-1}(E)} \left[\sum_{i=1}^{m-1} \frac{\partial \omega_i}{\partial a_{n-1}} + \alpha \frac{\partial \omega_m}{\partial a_{n-1}} \right] \qquad (3.16a)$$

$$\omega_i = \omega(E_i) = q_{n-1}(E_i(E)) / p'_n(E_i(E)) \qquad (3.16b)$$

$$\partial \omega_i / \partial a_{n-1} = \left[\{ q'_{n-1} p_{n-1} + \omega_i \; (p'_{n-1} p'_n - p_n p'_{n-1}) \} / \{ p'^2_n \} \right]_{E=E_i} \qquad (3.16c)$$

If α is a function of E, the above expressions are then modified and the library routines can be used as they stand as the output contains all information needed in the generalisation.

Sometimes it is useful to evaluate $\omega(E)$ without explicit calculation of a_i, then the Christoffel-Darboux theorem (Chihara, 1978) enables us to write a norm independent form:

$$\omega(E) = \frac{P_{n-2}(E)q_{n-2}(E) - P_{n-1}(E)q_{n-3}(E)}{P_{n-2}(E)p'_{n-1}(E) - p'_{n-2}(E)p_{n-1}(E) + p^2_{n-1}(E)/b^2_{n-1}} \qquad (3.17)$$

3.3 APPLICATION TO d-STATES:

Let us consider the one electron treatment of the d-bands of an fcc metal, say Nickel. The states of the system are the five atomic-like orbitals with d-symmetry on each atom. They are taken to be orthogonal to other orbitals on other sites. The Hamiltonian describes hopping of an electron from atom to atom induced by overlap of orbitals on one site with the potential of a nearest neighbour site. This hopping is described by the three Slater-Koster parameters $dd\sigma$, $dd\pi$ and $dd\delta$. The elements of H, that is, hopping parameters between orbitals on nearest neighbour atoms, are determined by performing the appropriate rotation, obtaining values that in general depend on $dd\sigma, dd\pi, dd\delta$. We approximate the crystal by a cluster of four unit cells of fcc lattice, containing 62 atoms.

In order to model the behavior of a d-electron in an infinite crystal, we choose initial states in the center of the cluster as having an environment most like the crystal. In an infinite fcc crystal, d-orbitals can be chosen

TABLE 3.1 Orbital Parameters for d Electrons in an Ion Crystal

n	a_n	b_n	a_n	b_n
	Orbital 1		Orbital 4	
0	0.0	0.100000E + 01	0.0	0.100000E + 01
1	−0.731282E − 02	0.295643E − 02	−0.262667E − 02	0.231155E − 02
2	−0.285673E − 01	0.235335E − 02	−0.833132E − 02	0.158428E − 02
3	−0.160738E − 01	0.139840E − 02	−0.962267E − 02	0.121493E − 02
4	−0.134218E − 01	0.162690E − 02	−0.545195E − 02	0.601881E − 03
5	−0.132190E − 01	0.156254E − 02	−0.472927E − 02	0.131840E − 02
6	−0.131124E − 01	0.174530E − 02	−0.398538E − 02	0.869993E − 03
7	−0.671958E − 02	0.153999E − 02	−0.611713E − 02	0.195845E − 03
8	−0.165180E − 01	0.155674E − 02	−0.219311E − 02	0.854633E − 03
9	−0.123618E − 01	0.173710E − 02	−0.107605E − 01	0.126903E − 02
10	0.0	0.168461E − 02	0.0	0.125162E − 02
	Orbital 2		Orbital 5	
0	0.0	0.100000E + 01	0.0	0.100000E + 01
1	−0.736282E − 02	0.295643E − 02	−0.262665E − 02	0.231155E − 02
2	−0.285674E − 01	0.235335E − 02	−0.833131E − 02	0.158428E − 02
3	−0.203862E − 01	0.205787E − 02	−0.116066E − 01	0.121205E − 02
4	−0.134732E − 01	0.152931E − 02	−0.126611E − 02	0.610531E − 03
5	0.907024E − 03	0.164361E − 02	−0.736555E − 02	0.135926E − 02
6	−0.596852E − 02	0.155990E − 02	−0.164093E − 02	0.985864E − 03
7	−0.463769E − 02	0.131672E − 02	−0.532776E − 02	0.824151E − 03
8	−0.128520E − 01	0.134450E − 02	−0.453183E − 04	0.955992E − 03
9	0.128076E − 02	0.160917E − 02	−0.123153E − 01	0.127544E − 02
10	0.0	0.158257E − 02	0.0	0.147469E − 02
	Orbital 3			
0	0.0	0.100000E + 01		
1	−0.736282E − 02	0.295643E − 02		
2	−0.285673E − 01	0.235335E − 02		
3	−0.203862E − 01	0.205787E − 02		
4	−0.134732E − 01	0.152932E − 02		
5	0.907022E − 03	0.164361E − 02		
6	−0.596851E − 02	0.155990E − 02		
7	−0.463773E − 02	0.131672E − 02		
8	−0.128520E − 01	0.134450E − 02		
9	0.128075E − 02	0.160917E − 02		
10	0.0	0.158227E − 02		

so that there are only that are non-equivalent : one coupling to the E_g states and the other coupling to the T_{2g} states. The cluster selected does not possess the full point group symmetry of the fcc lattice. The T_{2g} symmetry is split by the cluster boundary into a doublet and a singlet while the E_g doublet is also split.

Table 3.1 lists parameters for the first 11 levels for chains initiated by each of the five orbitals on the central atom of the cluster. There are a total of 310 degrees of freedom which is quite modest for a calculation of this type but serves for illustration. The chains have not terminated but considerable information can be derived from them. The first few levels of the chains display the triply degenerate T_{2g} and the doubly degenerate E_g symmetries. This is because until the chain states involve atoms on the boundary of the cluster,they have the full point group symmetry of the lattice. At the third level,the boundary splits the two lattice symmetries and this enables us to see the effect of the boundary. There is little to learn from the chain states except that because the Hamiltonian involves only nearest neighbour hopping, the weight of the states moves outward with each level until the states hit the boundary and scatter off it. The behaviour of the states is analogous to the free electron example, although the medium is discrete rather than continuous.

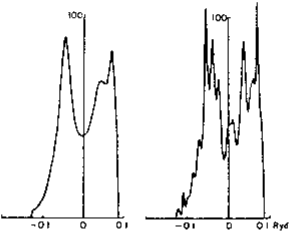

(a) (b)

Fig. 3.1 The fcc d bad local density of states as derived from a recursion method calculation on a cluster of ≃ 1000 atoms usinng (a) 5 and (b) 20 levels, respectively of the continued fraction expansion.

3.31 THE d BAND DENSITY OF STATES OF NICKEL

Figures 3.1 (a) and (b) show the d band density of states of pure Nickel as derived from a recursion method calculation on a cluster of ~ 1000 atoms using 5 and 20 levels respectively, of the continued fraction expansion. The centre of the band is near the zero of the energy scale for the up band of Nickel. The band starts from about -0.1 Ryd and continues upto 0.1 Ryd. The down band is however shifted slightly to the right (about 0.02 Ryd). The starting values of the band centres were taken from Hasegawa and Kanamori (1971).The scale used in their calculation was however different from the one used in the Recursion methd. We therefore utilised a conversion scale: $E^{REC} = 0.1 * E^{HAS} + 0.077$ for converting different energy values from Hasegawa scale to the Recursion scale. The Fermi level for Nickel in the Recursion was at 0.077 whereas in the Hasegawa it was at zero. The band centres were later self consistently calculated.

CHAPTER IV

ELECTRON CORRELATION IN NARROW ENERGY BANDS

4.1 INTRODUCTION

Transition and rare earth metals have in addition to their conduction bands, partly filled d or f-bands, which give rise to the characteristic properties of these metals. Correlation phenomena are of great importance in determining the properties of these narrow energy bands, indeed more important than the corresponding effects in conduction bands. Since these d or f-electrons are relatively more localised i.e. the band widths are narrower than the conduction bands, the free electron gas does not provide a good model for these bands. Therefore, a theory of correlation which adequately takes into account the atomistic nature of the solid is required. In the case of f-electrons of rare-earth metals, for most purposes a purely atomic (also referred to as Heitler-London or Localized) model will suffice. The same is not true for the d-electrons of the transition metals. Similarly correlation effects in a fully free electron gas

also is rather different in nature from the correlation effects in narrow energy bands.

The electron charge density in d-band is dense near the ion cores of the solid and sparse between them, that is why it is possible to assign an electron to a particular atom. This situation gives rise to the possiblility of an localised description of the d-band despite its band-width.

Experimentally, it has been observed that the d-electrons of the transition metals exhibit characteristics of both ordinary band model and the atomic model. Therefore, a theory of correlation in d-bands (in transition metals) should try to strike a balance between band like and atomic like behaviour.

In its simplistic form, the atomic theory pictures a transition metal as a collection of (say singly charged) ions immersed in the conduction electron gas and interacting with each other in much the same way as the correspondidng ions in salts. If the effective number of d-electrons is non-integral ,this simple picture breaks down. However, it is possible to substitute for it a less restrictive model which nevertheless guarantees most of the characteristic properties of the atomic model. It is sufficient to assert that, despite the band motion of d-electrons, the electrons on any atom are strongly correlated with each other but only

weakly with electrons on other atoms.Such intra-atomic correlations are inevitably make the metal behave to some extent according to the predictions of the atomic model.

The situation can be made clear by considering an example. Let us first consider a partly filled d-band of non-interacting electrons. In such a system the spin of an atom (that is, the total spin of all the electrons on that atom) is a quantity which fluctuates randomly in magnitude and direction.The characteristic time of fluctuation is of the order of the d-electron hopping time that is, the time in which a d-electron hops from one atom to another in the course of its band motion ($\tau \simeq \hbar/\Delta$ where Δ is the d electron band width). In this situation, one can think of spin being associated with each of the moving d-electrons.

We now switch on the electronic interaction. Hund's first rule for atoms which says that the intra-atomic interactions align the electron spins on an atom, will be useful since a similar effect in a metal is expected. Let us suppose now that the electrons have their spins quantized in what will be called the up and down directions and that at some instant a given atom has its total spin in the up direction. Then, by Hund's rule,the intra-atomic interactions are of such a nature that this atom tends to attract electrons with up spin and repel those with down spin. In

this way the property of an atom having a given total spin at some instant tends to be self perpetuating. If these intra-atomic forces are strong enough to produce appreciable correlations, then it follows that the state of total spin up on an atom may persist for a period long as compared to the d-electron hopping time. This persistence of the atomic spin state is not due to the same up spin electron being localized on the atom. The actual electrons on the atom are always changing as a result of their band motion, but the electron motions are correlated in such a way as to keep a preponderance of up spin electrons on the atom. In these circumstances (i.e. when the correlations are strong enough) one can think of the the spin as being associated with the atom rather than with the electrons and the possibility of an atomic or Heisenberg model emerges.

The above example illustrates the possibilities of the situation. Thus one may still assume the electrons to move rapidly from atom to atom as assumed in the band model, their motion may be correlated in such a manner as to give properties characteristic of the atomic theory. That is how the electrons can exhibit both types of behaviour simultaneously. The degree of atomic behaviour exhibited depends upon the strength of the correlations.

Thus an important requirement of a theory of correlation in narrow energy bands is that it has the

property of reducing to the atomic solution in the appropriate limit i.e. when applied to a hypothetical system of atoms on a lattice but widely separated from each other and interacting only weakly. Hubbard (1963) in his famous paper describes a very simple approximate theory fulfilling the above requirement. We describe his formulation below.

4.2 MATHEMATICAL FORMULATION

Let us consider a hypothetical partly filled narrow d-band containing n electrons per atom. The Bloch functions of the band will be denoted by ψ_k and the corresponding energy by E_k where k is the wave-vector. These wave functions and energies are assumed to have been calculated in some appropriate Hartree-Fock potential representing the average interaction of the d-band electrons with the electrons of the other bands besides the n electrons per atom of the d-band itself. The Hartree-Fock potential is assumed to be spin independent, as a result we have the same energies and wave functions for both spins.

We take $C_{k\sigma}$ and $C^{\dagger}_{k\sigma}$ to be the usual destruction and creation operators respectively for electrons in the Bloch state (k, σ) where $\sigma = \pm 1$ is the spin label. The dynamics of electrons of the band is represented approximately by the Hamiltonian

$$H = \sum_{k,\sigma} E_k \, C^{\dagger}_{k\sigma} C_{k\sigma} + \frac{1}{2} \sum_{\substack{k_1 k_2 \\ k_1' k_2'}} \sum_{\sigma_1 \sigma_2} \langle k_1 \, k_2 | 1/r | k_1' \, k_2' \rangle$$

$$\times \, C^{\dagger}_{k_1\sigma_1} \, C^{\dagger}_{k_2\sigma_2} C_{k_2'\sigma_2} \, C_{k_1'\sigma_1}$$

$$- \sum_{kk'} \sum_{\sigma} \left\{ 2 \langle kk' | 1/r | k'k \rangle \right\} \nu_{k'} C^{\dagger}_{k\sigma} C_{k\sigma} \qquad (4.1)$$

where $\mathbf{k}$ runs over the first Brillouin zone and

$$\langle k_1 k_2 | 1/r | k_1' k_2' \rangle = e^2 \int \frac{\psi^*_{k_1}(\vec{r}) \psi_{k_1'}(\vec{r}) \psi^*_{k_2}(\vec{r}') \psi_{k_2'}(\vec{r}')}{|\vec{r} - \vec{r}'|} \, d^3 r' \qquad (4.2)$$

The first term in (4.1) represents the band energy of the electrons and the second their interaction energy. The last term subtracts the potential energy of the electrons in that part of the Hartree-Fock field arising from the electrons of the d-band itself. The third term in equation (4.1) is there in order to avoid counting the interactions of the electrons of the band twice:once explicitly in the Hamiltonian and then implicitly through the Hartree Fock field determining E_k. The ν_k are the assumed occupation

numbers of the states of the band in the Hartree Fock calculation, assuming up and down spin states to be occupied equally.

It is now convenient to go over to a tight binding representation of the Hamiltonian by taking recourse to the Wannier functions

$$\phi(\vec{r}) = N^{-1/2} \sum_k \psi_k(\vec{r}) \qquad (4.3)$$

where N is the number of atoms. One can write

$$\phi_k(\vec{r}) = N^{-1/2} \sum_i e^{i\vec{k}.\vec{R}_i} \phi_i(\vec{r}-\vec{R}_i) \qquad (4.4)$$

where the sum runs over all the atomic positions $\vec{R}_i$. Introducing the creation and destruction operators $C^{\dagger}_{i\sigma}$ and $C_{i\sigma}$ for an electron of spin σ in the orbital state $\phi_i(\vec{r}-\vec{R}_i)$. One can write

$$C_{k\sigma} = N^{-1/2} \sum_i e^{i\vec{k}.\vec{R}_i} C_{i\sigma} \quad ; \quad C^{\dagger}_{k\sigma} = N^{-1/2} \sum_i e^{-i\vec{k}.\vec{R}_i} C^{\dagger}_{i\sigma} \qquad \ldots\ldots (4.5)$$

Thus the Hamiltonian (4.1) can be rewritten as

$$H = \sum_{ij} T_{ij} C^{\dagger}_{i\sigma} C_{j\sigma} + \frac{1}{2} \sum_{\substack{i,j \\ k,\ell}} \sum_{\sigma,\sigma'} \langle ij|1/r|k\ell\rangle\, C^{\dagger}_{i\sigma}\, C^{\dagger}_{j\sigma'}\, C_{i\sigma'} C_{k\sigma}$$

$$- \sum_{ik\ell} \sum_{\sigma} \{2\langle ij|1/r|\ell k\rangle\} \nu_{j\ell}\, C^{\dagger}_{i\sigma}\, C^{\dagger}_{k\sigma} \qquad (4.6)$$

where, $$T_{ij} = N^{-1} \sum_{k} E_k\, e^{i\vec{k}.(\vec{R}_i - \vec{R}_j)} \qquad (4.7)$$

$$\langle ij|1/r|k\ell\rangle = e^2 \int \frac{\phi^*(\vec{r}-\vec{R}_i)\,\phi(\vec{r}-\vec{R}_k)\,\phi^*(\vec{r}\,'-\vec{R}_j)\,\phi(\vec{r}\,'-\vec{R}_\ell)}{|\vec{r}-\vec{r}\,'|} \times d^3\vec{r}\; d^3\vec{r}\,' \qquad (4.8)$$

and $$\nu_{j\ell} = N^{-1} \sum_{k} \nu_k\, e^{-i\vec{k}.(\vec{R}_j - \vec{R}_\ell)} \qquad (4.9)$$

We will now make the essential simplifying approximation. Since we are dealing with narrow energy bands the Wannier function ϕ will closely resemble atomic functions. Also, if the band width is small, these d-functions must form an atomic shell which has a radius small compared to the inter atomic spacing. From equation (4.8) it may be seen that in this circumstance the integral $\langle ii|1/r|ii\rangle = U$ will be much greater in magnitude than any of the other integrals (4.8), suggesting that all the integrals (4.8) maybe neglected in comparison to U. Making this approximation the Hamiltonian of (4.6) reduces to

$$H = \sum_{i,j} T_{ij} C^{\dagger}_{i\sigma} C_{j\sigma} + \frac{1}{2} U \sum_{i\sigma} n_{i\sigma} n_{i-\sigma}$$

$$-U \sum_{i\sigma} \nu_{ii} n_{i\sigma} \qquad (4.10)$$

where $n_{i\sigma} = C^{\dagger}_{i\sigma} C_{i\sigma}$. From (4.9) $\nu_{ii} = N^{-1} \sum_{k} \nu_{k} = n/2$

So, the last term of equation (4.10) reduces to

$$-\frac{1}{2} Un \sum_{i\sigma} n_{i\sigma} = -\frac{1}{2} Un^{2} = \text{Const.}$$

and may, therefore, be dropped after a redefinition of the zero of our energy scale. Equation (4.10) is the approximate Hamiltonian used hereafter.

Many approximations have been made in the derivation of the simplified Hamiltonian (4.10). We will now examine the validity of these approximations as applied to the case of 3d-electrons in the transition metals.

The most obvious approximation has been the neglect of all the interaction terms in equation (4.6) other than U. For the sake of comparison, one has to note that U has the order of magnitude $\simeq$ 20 eV for 3d electrons in transition metals. The largest of the neglected terms are those of the type $\langle ij|1/r|ij\rangle$ where i and j are nearest neighbours. From

(4.8) these integrals can be estimated to have the order of magnitude $(2/R)R_{ij} \approx 6$ eV (R = inter atomic spacing in Bohr units). This figure, however, gets reduced appreciably when we allow for the screening of the interactions of electrons on different atoms by the conduction electron gas. This screening effect is taken into account by multiplying the above estimate by a factor of $e^{-\lambda R}$ where λ is an appropriate screening constant. In the case of 3d-transition metals $e^{-\lambda R} \approx \frac{1}{3} - \frac{1}{2}$, reducing the $\langle ij|1/r|ij\rangle$ term to the order of magnitude 2 to 3 eV. For the case in which i and j are not nearest neighbours

$$\langle ij|1/r|ij\rangle \approx \frac{2e^{-\lambda \cdot |\vec{R}_i - \vec{R}_j|}}{|\vec{R}_i - \vec{R}_j|} R_{ij}$$

which falls off rapidly with increasing $|\vec{R}_i - \vec{R}_j|$, on account of the exponential factor. Thus the term

$$\frac{1}{2} \sum_{i,j} \sum_{\sigma\sigma'} \langle ij|1/r|ij\rangle \, n_{i\sigma} n_{j\sigma'} \qquad (4.11)$$

in equation (4.6) can perhaps be neglected as compared to U as a first approximation.

The other neglected terms are of the type

$$\langle ii|1/r|ij\rangle \simeq q \text{ Ryd} \simeq 0.5 \text{ eV}$$

$$\langle ij|1/r|ik\rangle \simeq \frac{1}{4}\, q \text{ Ryd} \simeq 0.1 \text{ eV}$$

$$\langle ii|1/r|jj\rangle \simeq \langle ij|1/r|ji\rangle \simeq q^2 \text{ Ryd} \simeq 0.025 \text{ eV}$$

where i, j and k are all nearest neighbours, and $q \simeq 0.05$ is the overlap charge (in units of e) between two 3d-electrons on nearest neighbour atoms. All other interaction terms in equation (4.6) which have been neglected are still smaller than those which one sees are already small compared to those of equation (4.11)

Another approximation that has been made use of is that only the interactions among 3d-electrons is considered, the interaction with electrons of the other bands being represented only through the Hartree-Fock field. In estimating the order of magnitude of the terms of equation (4.11) due allowance was made for the screening effects of the conduction electron gas on the interactions. So, the question arises as to whether there is a similar screening effect reducing the margin of U. There is, in fact, such an effect. The speed with which d-electrons move from atom to atom is slow compared to the velocity of a typical conduction electron and, therefore, the latter can correlate efficiently with the d-electrons and screen their fields. Thus, if a given atom has an extra d-electron, its negative charge will repel conduction electrons producing a correlation hole about atom in the conduction electron gas. The presence of this

hole reduces the electrostatic potential at the atom (and, therefore, at each of its d-electrons) by about 5 eV which is the same thing as reducing U by 5 eV. This reduction though appreciable does not change the order of magnitude of U.

There is also a reduction in U by the screening of the interactions of the d-electrons by the core electrons and by the d-electrons themselves. This, however, is not a big effect because the kinetic energies of the orbital motion of the d-electrons are large compared to U. One can estimate the reduction in U due to this effect by noticing that a similar effect will occur in free atoms. In the latter case (free atoms) it has been found that these effects make the F^2(3d, 3d) and F^4(3d, 3d) parameters [using the notation of Condon and Shortley (1935)] determined from experiment about 10 to 20 % smaller than those calculated from Hartree Fock wave functions (Watson 1960). So one may expect a reduction in U of a similar order of magnitude.

It appeared more reasonable to use in the Hamiltonian of equation (4.10) an effective U ($\sim$ 10 eV) rather than that given by the integral (4.8). The approximations involved in equation (4.10) are otherwise not so poor as to make it an unreasonable starting point for a theory of correlations for the d-band electrons. The terms omitted in going from (4.6) to (4.10) may be treated as perturbations on the solutions obtained from (4.10).

4.3 THE HARTREE-FOCK APPROXIMATION

One can obtain the effective Hartree-Fock Hamiltonian by linearizing the interaction terms in the true Hamiltonian. In our Hamiltonian (4.10) this is achieved by simply replacing the term $n_{i\sigma}n_{i\bar{\sigma}}$ by $\frac{1}{2}\,[\,n_{i\sigma}\langle n_{i\bar{\sigma}}\rangle + n_{i\bar{\sigma}}\langle n_{i\sigma}\rangle]$, where $\langle n_{i\sigma}\rangle$ is the average of the expectation of $n_{i\sigma}$ over a canonical ensemble at some temperature . Dropping the last term of (4.10) (anyway a constant), the Hartree-Fock Hamiltonian is reduced to

$$H = \sum_{i,j} T_{ij}\, C^{\dagger}_{i\sigma}\, C_{j\sigma} + U \sum_{i,\sigma} n_{i\sigma}\, \langle n_{i\bar{\sigma}}\rangle \qquad (4.12)$$

Restructuring to the class of solutions for which

$$\langle n_{i\sigma}\rangle = n_{\sigma} \text{ for all } i \qquad (4.13)$$

Eqn. (4.12) reduces to

$$H_{hf} = \Sigma\, T_{ij}\, C^{\dagger}_{i\sigma}\, C_{j\sigma} + U \sum_{i,\sigma} n_{-\sigma}\, C^{\dagger}_{i\sigma}\, C_{i\sigma} \qquad (4.14)$$

Transforming back to the operators $C^{\dagger}_{k\sigma}\, C_{k\sigma}$

$$H_{hf} = \sum_{k} \sum_{\sigma} \{E_k + U\, n_{-\sigma}\}\, C^{\dagger}_{k\sigma}\, C_{k\sigma} \qquad (4.15)$$

This is simply the Hamiltonian for a collection of non-interacting electrons with a slightly modified band structure, the energy of the (k,σ) state now being $(E_k+U\,n_{-\sigma})$ rather than E_k. If $\rho(E)$ represents the density of states per atom corresponding to the band structure E_k, then the densities of state $\rho_\sigma(E)$ where $\sigma = \pm 1$ for the electrons described by the Hamiltonian of (4.15) are

$$\rho_\sigma(E) = \rho(E-Un_{-\sigma}) = \rho(E-Un + Un_\sigma) \qquad (4.16)$$

where the last term follows from

$$n_\uparrow + n_\downarrow = n \qquad (4.17)$$

If μ is the chemical potential of the electrons then at the absolute zero of temperature, one has

$$n_\sigma = \int_{-\infty}^{\mu} \rho_\sigma(E)\,dE = \int_{-\infty}^{\mu} \rho\,(E - U\,n + U\,n_\sigma)dE \qquad (4.18)$$

The pair of equations (4.18) must now be solved together with (4.17) for $n_\uparrow$, $n_\downarrow$ and μ.

One possible solution of equation (4.18) is when

$$n_\uparrow = n_\downarrow = n/2 \qquad (4.19)$$

which represents a non magnetic state of the system : μ is determined by

$$n/2 = \int_{-\infty}^{\mu} \rho(E - \frac{1}{2} U n)\, dE \qquad (4.20)$$

It may be possible to find ferromagnetic solution even if $n_\uparrow \neq n_\downarrow$ provided U is sufficiently large. In this case equationn (4.18) must have two distinct solutions such that they satisfy equation (4.17).

It can be readily seen that the condition (4.19) and (4.20) give a double solution of (4.18). But this condition can at once be found from (4.18) to be

$$1 = U\, P(\mu - \frac{1}{2} Un) \qquad (4.21)$$

Thus, if for any E, the condition $U\ P(E) > 1$ is satisfied, then for some n and μ determined by (4.20) and (4.21) Hartree-Fock theory predicts that the system will become ferromagnetic. It will be found that when correlation effects are taken into account one obtains a somewhat more restrictive condition for ferromagnetism.

4.4 CPA AND CLUSTER CPA ADAPTED TO FERROMAGNETIC ALLOYS

In an alloy $A_c B_{1-c}$ having atoms A and B distributed in a random manner, the Hiamiltonian is given by

$$H = \sum_{i\sigma} \varepsilon_i a^{\dagger}_{i\sigma} a_{i\sigma} + \sum_{\sigma, i, j(\neq i)} V_{ij} a^{\dagger}_{i\sigma} a_{j\sigma} + \sum_i U_i a^{\dagger}_{i\sigma} a_{i\sigma} a^{\dagger}_{i-\sigma} a_{i-\sigma} \qquad (4.22)$$

where $a^{\dagger}_{i\sigma}$, $a_{i\sigma}$ are the creation and annihilation operators respectively of an electron with spin σ = ($\uparrow$ or $\downarrow$) of the Wannier orbital at the i^{th} lattice site. ε_i is the average energy of an electron at the i^{th} lattice site taking values ε_A and ε_B depending upon whether A atom or B atom occupies the i^{th} lattice site. V_{ij} in the second term represents the transfer integral between the sites i and j which we assume to be independent of the species of atoms occupying these sites. U_i in the last term is the Coulomb integral of the electrons, taking values U_A or U_B depending on the atoms on the i^{th} lattice sites. We assume that the parameters ε_A, ε_B, V_{ij}, U_A and U_B are independent of the concentration of the given alloy $A_c B_{1-c}$.

The Hamiltonian (4.22) is an adaptation of the Hamiltonian proposed by Velický *et al* (1968) to ferromagnetic alloys for a single band model. The Coulomb interaction term introduced in the Hamiltonian following the model assumed by

Hubbard (1963) and Kanamori (1963) in their discussions of the electron correlation. The assumption of non-randomness of the V_{ij} means that the band shape in pure metal A is the same as that in pure metal B . For the alloys, having the transition metals as their constituents, the Hamiltonian given by (4.22) will represent the essential aspects of the electronic structure. Besides the Hamiltonian is the simplest among the conceivable models.

Using the Hartree-Fock approximation discussed in the earlier chapter, we write the effective Hamiltonian H_σ for electrons with spin σ as

$$H_\sigma = \sum_i \varepsilon_{i\sigma}\, a^\dagger_{i\sigma}\, a_{i\sigma} + \sum_{ij} V_{ij}\, a^\dagger_{i\sigma}\, a_{j\sigma} \qquad (4.23)$$

where $\varepsilon_{i\sigma} = \varepsilon_i + U_i \langle a^\dagger_{i-\sigma}\, a_{i-\sigma}\rangle$ (4.24)

where $\langle a^\dagger_{i-\sigma}\, a_{i-\sigma}\rangle = n_{i-\sigma}$ is the average number of electrons with spin $-\sigma$ at the i^{th} lattice site. The average number will be given by

$$\langle a^\dagger_{i-\sigma}\, a_{i-\sigma}\rangle = n_{i-\sigma} \qquad (4.25)$$

where i = A or B.

In a realistic model we should consider a multi-band case, rather than the single band case we have

been discussing so far. In this case, the one electron Hamiltonian for the given alloy is assumed to have the form

$$H = \sum_{i\mu\sigma} \varepsilon_{i\mu\sigma} \; a^{\dagger}_{i\mu\sigma} a_{i\mu\sigma} + W \qquad (4.26)$$

with, $\varepsilon_{i\mu\sigma} = \varepsilon_i + U_{i\mu} < a^{\dagger}_{i\mu-\sigma} a_{i\mu-\sigma}>$

$$+ \sum_{\sigma',\mu'(\neq\mu)} U_{i\mu\mu'} <a^{\dagger}_{i\mu'\sigma'} a_{i\mu'\sigma'}>$$

$$- \sum_{\mu'(\neq\mu)} J_{i\mu\mu'} <a^{\dagger}_{i\mu'\sigma} a_{i\mu'\sigma}> \qquad (4.27)$$

where μ stands for one of the degenerate bands and the corresponding atomic orbital. Other subscripts are the same as in the case of nondegenerate band. $U_{i\mu\mu'}$ and $J_{i\mu\mu'}$ are the on site Coulomb and exchange integrals between different orbitals labelled by μ and μ'. We represent that part of the Hamiltonian which gives rise to the state density $\rho^{(0)}(\varepsilon)$ for all μ and σ. For simplicity we assume that the Coulomb integrals are the same for all i, μ and μ' i.e. $U_{i\mu\mu'} = U_{i\mu} = U$ and similarly the exchange integrals between different orbitals are of the same magnitude $J_{i\mu\mu'} = J$. We assume that $n_{i\sigma} = <a^{\dagger}_{i\mu\sigma} a_{i\mu\sigma}>$ is the same for all μ. $\varepsilon_{i\mu\sigma}$ which is now independent of μ is given by

$$\varepsilon_{i\mu\sigma} = \varepsilon_{i\sigma} = \varepsilon_i + U n_{i-\sigma} + \sum_{\mu'(\neq\mu)} U\, n_{i\mu'-\sigma} + \sum U\, n_{i\mu'\sigma}$$

$$- \sum J\, n_{i\mu'\sigma}$$

$$= \varepsilon_i + U\, n_{i-\sigma} + 4\, U n_{i-\sigma} + 4\, U\, n_{i\sigma} - 4\, J n_{i\sigma}$$

$$= \varepsilon_i + 5U\, n_{i-\sigma} + 4\,(U-J)\, n_{i\sigma}$$

$$= \varepsilon_i + 5U n_{i-\sigma} + 4\,(U-J)(n - n_{i-\sigma})$$

$$= \varepsilon_i + 5U n_{i-\sigma} - 4(U-J) n_{i-\sigma} + 4(U-J) n$$

$$= \varepsilon_i + U n_{i-\sigma} + 4\, J n_{i-\sigma} + \text{Const}$$

(redifining the zero of the energy again)

$$= \varepsilon_i + (U+4J)\, n_{i-\sigma} \qquad (4.28)$$

In the coherent potential approximation the average number of electrons at a site does not depend on the site, though it depends on the species of atoms occupying the site. The average numbers $n_{A\sigma}$ or $n_{B\sigma}$ will be calculated self consistently by the use of the formula given below.

In our problem, the coherent potential is spin dependent and so it will be represented by Σ_σ. While ε_A and ε_B are replaced by $\varepsilon_{A\sigma}$ and $\varepsilon_{B\sigma}$, to obtain the necessary formulas from Velicky *et al* (1968) paper. Thus the coherent potential Σ_σ which is a function of z where $z = \varepsilon + i\delta$ should satisfy for a given concentration c and 1-c

$$c\,\varepsilon_{A\sigma} + (1-c)\,\varepsilon_{B\sigma} - \Sigma_{\sigma}(z)$$

$$= \{\varepsilon_{A\sigma} - \Sigma_{\sigma}(z)\}\; G_{\sigma}(z)\{\varepsilon_{A\sigma} - \Sigma_{\sigma}(z)\} \qquad (4.29)$$

where $G_{\sigma}(z)$ is given by

$$G_{\sigma}(z) = G^{(0)}(z - \Sigma_{\sigma}(z))$$

$$= \int_{-\infty}^{\infty} \frac{\rho^{(0)}(\varepsilon)}{z - \Sigma_{\sigma}(z) - \varepsilon}\, d\varepsilon \qquad (4.30)$$

where $\rho^{(0)}(\varepsilon)$ is the density of states per unit energy defined for the energy band given by the second term in the right hand side of the equations (4.22) and (4.23). The average number of electrons on the atoms A or B is calculated by the relation

$$n_{i\sigma} = \int_{-\infty}^{\infty} \rho_{i\sigma}(\varepsilon)\, f(\varepsilon)\, d\varepsilon \qquad (4.31)$$

where i = A or B

where $f(\varepsilon)$ is the Fermi distribution function at a given temperature T,

$$f(\varepsilon) = \frac{1}{1 + \exp\{(\varepsilon - \mu)/kT\}} \qquad (4.32)$$

$\rho_{i\sigma}(\varepsilon)$ is the energy distribution function of electrons on atom i given by

$$\rho_{i\sigma}(\varepsilon) = -\frac{1}{\pi}\,\mathrm{Im}\left[\frac{\langle G_{\sigma}(z)\rangle}{\{1-(\varepsilon_{i\sigma}-\Sigma_{\sigma}(z))\,\langle G_{\sigma}(z)\rangle\}}\right] \qquad (4.33)$$

where $z \longrightarrow \varepsilon + i\delta$

In the case of CCPA, we embed a cluster of atoms in the effective medium. We demand, that there is no extra scattering on the average as a result. As in 1CPA, we find the self energy Σ self consistently. In CCPA, however, Σ will be a matrix with components between sites within the cluster. Having self consiatently calculated $\underline{\Sigma}$ and also the configurationally averaged Green function for both up and down case, the partial density of states $\rho_{i\sigma}(\varepsilon)$ will be given as

$$\langle\rho_{i\sigma}(\varepsilon)\rangle = -\frac{1}{\pi}\,\mathrm{Im}\left[\frac{\langle G_{\sigma}(z)\rangle}{\{1-(\varepsilon_{i\sigma}-\Sigma_{\infty\sigma}(z))\langle G_{\sigma}(z)\rangle\}}\right] \qquad (4.33a)$$

i = A or B

$z \longrightarrow \varepsilon + i\delta^{+}$

For the 2CPA, $\underline{\Sigma}$ has two independent elements Σ_0 and Σ_1, one diagonal and the other off-diagonal. The self-energies are determined self-consistently within the augmented space formalism discussed in Chapter II.

For practical calculations we select parameters

ε_A, ε_B, U_A, U_B and the state density function $\rho^{(0)}(\varepsilon)$ as the input. We determine six unknown quantities $n_{i\sigma}$ (i = A or B) and $\sigma = \uparrow$ or $\downarrow$ and Σ_σ through six simultaneous transcendental equations.

After solving the simultaneous equations (4.29) to (4.33) we obtain various physical quantities of the alloy. The density of states of electrons with spin σ is

$$\rho_\sigma = c\,\rho_{A\sigma} + (1-c)\,\rho_{B\sigma} \tag{4.34}$$

The average number of electrons with spin σ per atom is given by

$$n_\sigma = c\,n_{A\sigma} + (1-c)\,n_{B\sigma} \tag{4.35}$$

The magnetic moment of A or B atom in the units of μ_B is obtained by

$$m_i = 5\,(n_{i\uparrow} - n_{i\downarrow}) \qquad (i = A \text{ or } B) \tag{4.36}$$

the factor 5 accounts for the five fold degeneracy of the actual d-bands. The average magnetic moment of the alloy per atom in the same unit is given by

$$m = c\,m_A + (1-c)\,m_B \tag{4.37}$$

There are, as usual, two nested self-consistency loops. With a given choice for $n_{i\sigma}$ we fix our $\varepsilon_{i\sigma}$ and carry out the CCPA calculation for the averaged Green functions $\langle G_{\sigma}(z) \rangle$ as described in Chapter II. This involves a self-consistent evaluation of $\underline{\Sigma}_{\sigma}$. Then we recalculate $n_{i\sigma}$ and μ using (4.31) and then iterate till self-consistency is achieved.

We should note that we have set out to generalise the augmented space approach to cases which require a self-consistent determination of the Hamiltonian. We have achieved this in this section in its application to a simple model. The final object will be to demonstrate an actual implementation of this to a canonical example.

4.5 APPLICATION TO Ni_{1-c} Fe_{c} SYSTEMS

In our calculation, we require $\rho^{(\sigma)}(\varepsilon)$ as an input. Hasegawa and Kanamori (1971) has taken a steeple model. We, however, take as our input the realistic density of states obtained from the recursion method as described in Chapter III. We have already described this calculation in the earlier chapter in some detail. This input is quantitatively far superior to the steeple model.

We will take, for pure nickel, 1.88 electrons per

atom per d-band and in pure iron 1.44 electrons per atom per d-band. In order to reduce the adjustable parameters, we will assume $U_A = U_B = U$. The U value is also adjustable. Hasegawa and Kanamori (1971) have taken U = 1.25 in units of a half of the band width of the pure metal. We have, however, in our multi band case, taken U to be 0.5 and J = 0.19 so that (U+4J) which approximately corresponds to U in the non degenerate case is equal to 1.26, which is very nearly equal to Hasegawa and Kanamori's U = 1.25 In our case (degenerate bands), $\varepsilon_{i\sigma}$ depends upon both $n_{i\sigma}$ and $n_{i-\sigma}$ unlike the degenerate case where $\varepsilon_{i\sigma}$ depends on $n_{i-\sigma}$ only. So long as $n_{i\sigma}+n_{i-\sigma}$ is kept constant this will introduce no greater difficulties.

In the practical calculation, we first start with appropriate guess values of $\varepsilon_{A\sigma}$, $\varepsilon_{B\sigma}$, $\varepsilon_{A-\sigma}$, $\varepsilon_{B-\sigma}$. With the help of equation (4.29) and (4.30), we self consistently find the value of $\langle G_\sigma(z)\rangle$ and $\Sigma_\sigma(z)$. Knowing these, we can calculate $\rho_{i\sigma}$'s and the corresponding $n_{i\sigma}$'s. The trial values of $n_{i\sigma}$'s which were used in the calculation of $\varepsilon_{i\sigma}$'s should be very near $n_{i\sigma}$'s thus calculated. The whole cycle of computation is iterated until the consistency between the trial values and calculated values of $n_{i\sigma}$'s are within a prechosen error bar. Knowing $n_{i\sigma}$'s, we proceed to find ρ_σ, the density of states with spin σ, n_σ the number of electrons with spin σ, the magnetic moment m_i of the i^{th} atom (i = A or

B) and finally m, the average magnetic moment of the alloy via equations (4.34) to equations (4.37) respectively.

Note that while the band centres for Ni and Fe are being self- consistently calculated, the band centre of Ni is kept effectively at zero for both up and down cases. The centre for Fe is correspondingly shifted. The $\langle G_\sigma(z)\rangle$s and $\Sigma_\sigma(z)$s for various energy values are calculated. The $n_{i\sigma}$'s are calculated after shifting the band centres back to their original positions. Also, due consideration is taken regarding the difference of the band centre for pure Ni in up and down cases. The component densities of states for both up and down cases are checked for normalisation. The magnetic moment calculations can be done only with the properly normalised density of states.

4.6 RESULTS AND DISCUSSION

Figures (4.1) and (4.2) show respectively the density of states per spin per unit energy for various concentrations of Fe in CPA and CCPA. It is obvious from the figuress (4.1) and (4.2) that for both CPA and CCPA the minority spin band (or down spin band) deforms itself considerably, whereas the majority spin band (or up spin band) more or less keeps its shape intact with changing concentrations of Fe in the alloy. Expectedly, in the CCPA

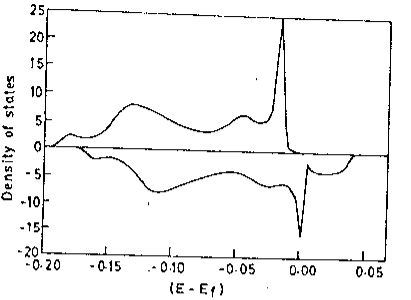

Fig. 4.1a Energy against component densities of states in CPA for c = 0.1

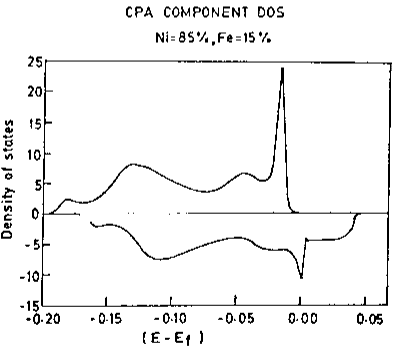

Fig. 4.1b Energy against component densities of states in CPA for c = 0.15

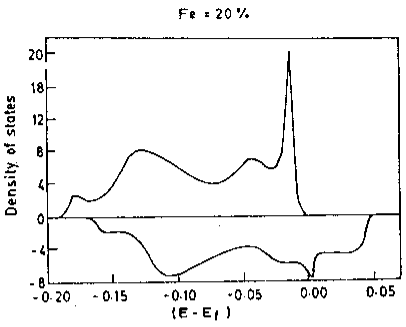

Fig. 4.1c Energy against component densities of states in CPA for c = 0.20

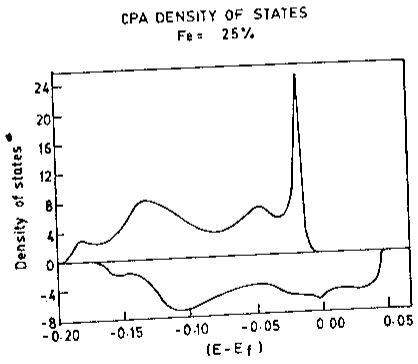

Fig. 4.1d Energy against component densities of states in CPA for c = 0.25

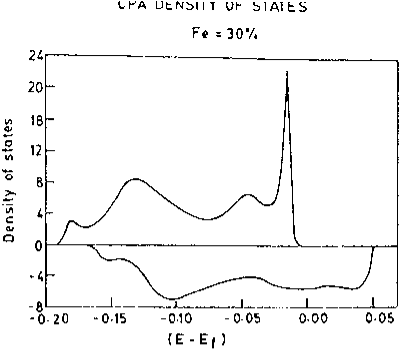

Fig. 4.1e Energy against component densities of states in CPA for c = 0.30

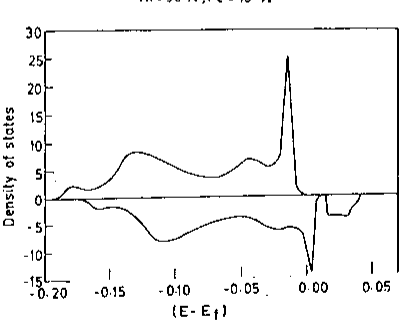

Fig. 4.2a Energy against component densities of states in CCPA for c = 0.10

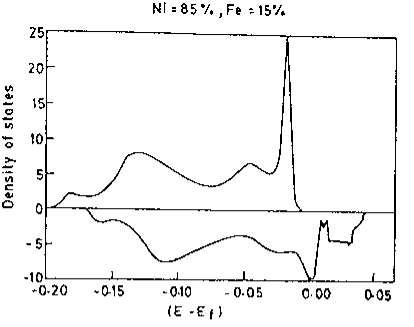

Fig. 4.2b Energy against component densities of states in CCPA for c = 0.15

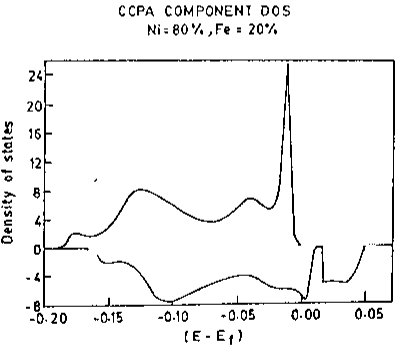

Fig. 4.2c Energy against component densities of states in CCPA for c = 0.20

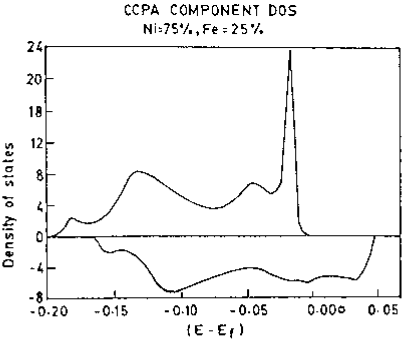

Fig. 4.2d Engy against component densities of states in CCPA for c = 0.25

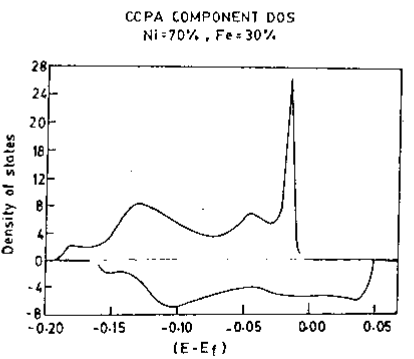

Fig. 4.2e Energy against component densities of states in CCPA for c = 0.30

(Fig 4.2), there are more structures in the down spin band. In both up and the down spin bands, we have a sharp peak in the vicinity of the Fermi level (towards the immediate left of the Fermi level in the up spin band and towards the immediate right of it in the down spin band.)

The deformation in the minority spin bands for various Fe concentrations in the alloy are due to the fact that the band centres of Ni and Fe are further apart in the minority spin bands than in the majority spin case where the band centres are very close to each other. The band centres of Ni and Fe for both up and down spins, can also be calculated from equation (4.28) provided the electron numbers for Ni and Fe for various concentrations of Fe are known. Hasegawa & Kanamori (1971) have given estimates of these quantities which they have used for their work.

Apart from the deformation in the minority spin band, another feature observed in figures (4.1) and (4.2) is that the peak observed in the minority spin band (to the right of Fermi level) gets widened with increasing concentration of Fe in the alloy. Also its height decreases gradually till the peak almost disappears into a shoulder at 20% of Fe concentration in the alloy. This is observed both in CPA as well as in CCPA. In the latter case, a impurity

subband appears in the minority band. The CPA already indicated the beginings of the subband splitting off. This subband merges into the minority band as the concentration of Fe increases to 25%.

In figures (4.3) and (4.4) we show the energy distribution of electrons at Ni and Fe sites (the partial densities of states) $\rho_{Ni\sigma}(\varepsilon)$ and $\rho_{Fe\sigma}(\varepsilon)$ for various Fe concentrations in CPA case. Figures (4.5) and (4.6) are their equivalents in the CCPA. Again, as in the case of component densities of states, the partial densities of states for both Fe and Ni in the majority spin state preserve their shape for various Fe concentrations. So much so that the partial densities of states for Fe and Ni at any concentration of Fe tally with one another so that they could not be shown distinctly in one figure. This, however, was not so in the minority spin states, where, even for a particular concentration of Fe in the alloy, Fe and Ni have very different shapes.

Another noticeable feature is that in the case of Ni, the peaks (corresponding to the two cases of spin up and spin down) are very close to each other on either side of the Fermi level. In the case of Fe, however, the corresponding peaks are separated by larger energy gaps. Also, unlike the case of partial density of states for Ni, in that for Fe, the

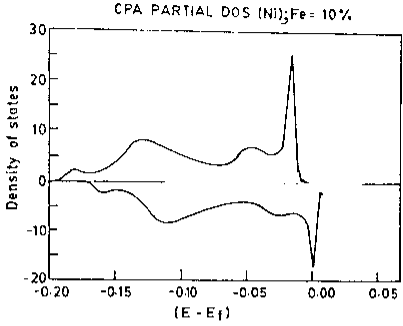

Fig. 4.3a Energy agsinst partial densities of states of Ni in CPA for c = 0.10

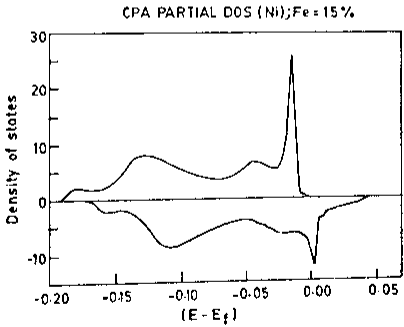

Fig. 4.3b Energy against partial densities of states of Ni in CPA for c = 0.15

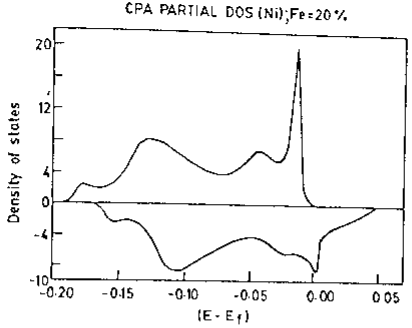

Fig. 4.3c Energy againnst partial densities of states of Ni in CPA for c = 0.20

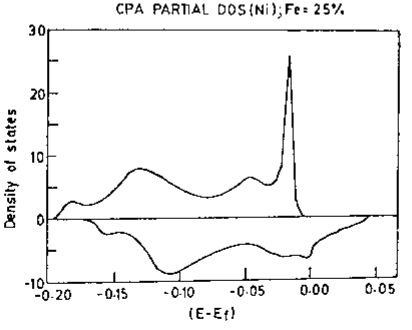

Fig. 4.3d Energy against partial densities of states of Ni in CPA for c = 0.25

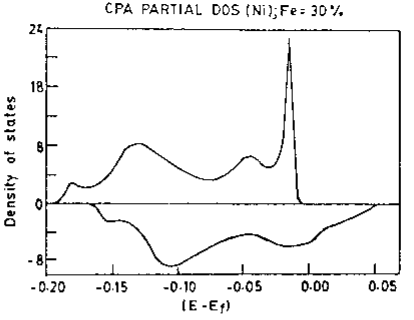

Fig. 4.3e Energy against partial densities of states of Ni in CPA for c = 0.30

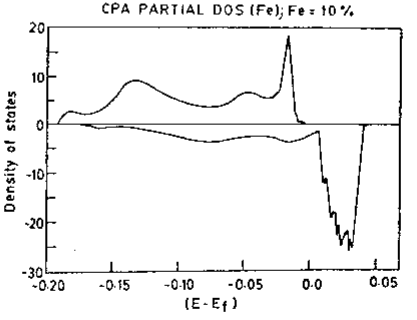

Fig. 4.4a Energy against partial densities of states of Fe in CPA for c = 0.10

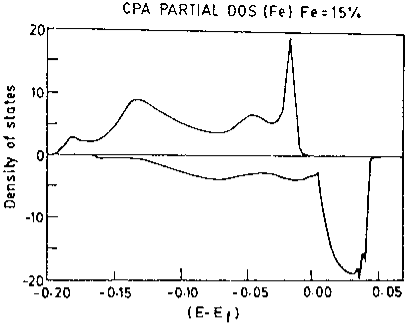

Fig. 4.4b Energy againnst partial desities of states of Fe in CPA for c = 0.15

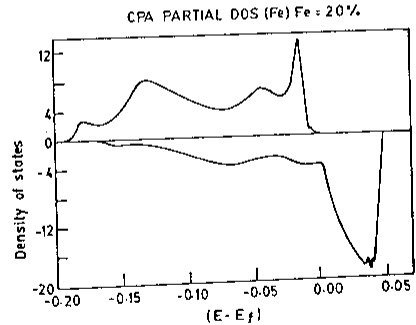

Fig. 4.4c Energy agaist partial densities of states of Fe in CPA for c = 0.20

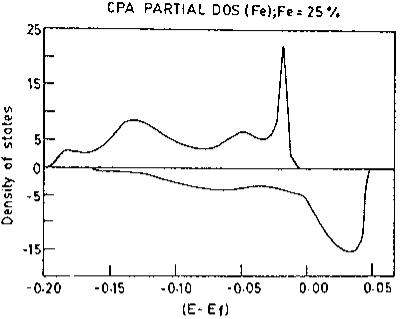

Fig. 4.4d Energy against partial densities of states of Fe in CPA for c = 0.25

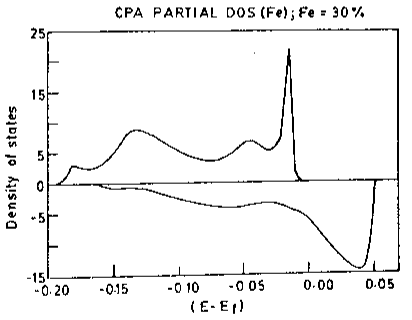

Fig. 4.4e Energy against partial densities of states of Fe in CPA for c = 0.30

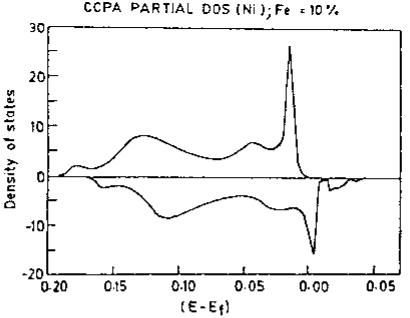

Fig. 4.5a Eergy against partial densities of states of Ni in CCPA for c = 0.10

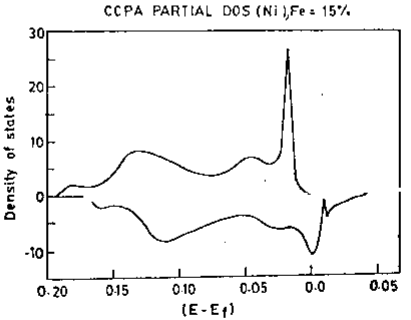

Fig. 4.5b Energy against partial densities of states of Ni in CCPA for c = 0.15

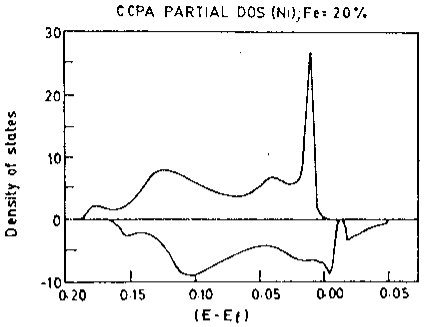

Fig. 4.5c Energy against partial desities of states of Ni in CCPA for c = 0.20

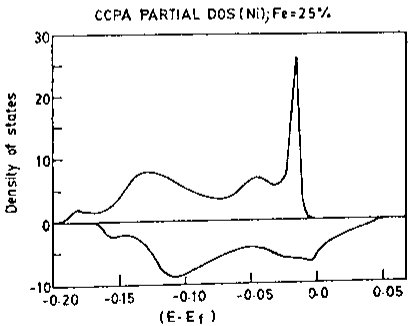

Fig. 4.5d Energy against partial densities of states of Ni in CCPA for c = 0.25

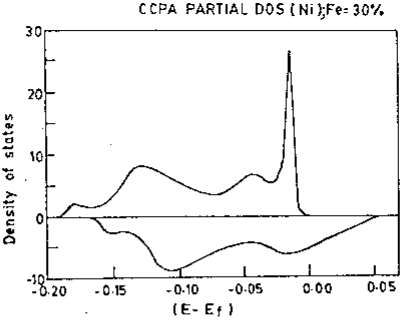

Fig. 4.5e Energy against partial densities of states of Ni in CCPA for c = 0.30

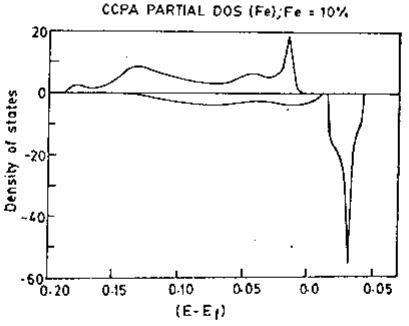

Fig. 4.6a Energy against partial densities of states of Fe in CCPA for c = 0.10

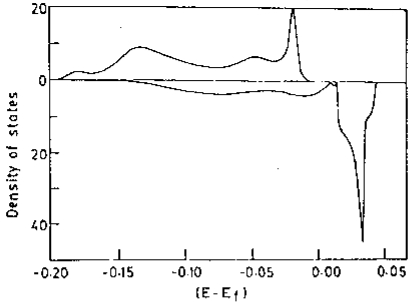

Fig. 4.6b Energy against partial densities of states of Fe in CCPA for c = 0.15

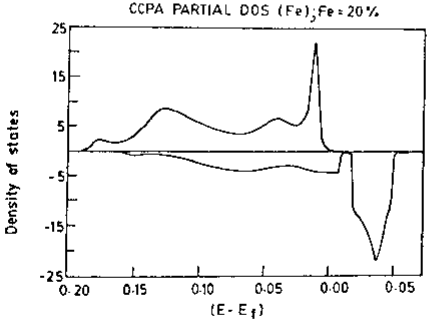

Fig. 4.6c Energy against partial densities of states of Fe in CCPA for c = 0.20

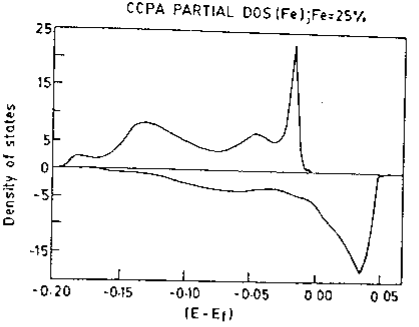

Fig. 4.6d Energy againnst partial densities of states of Fe in CCPA for c = 0.25

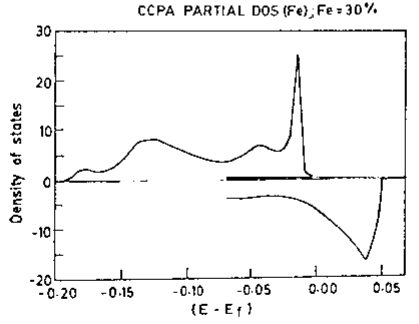

Fig. 4.6e Energy against partial densities of states of Fe in CCPA for c = 0.30

peak corresponding to the spin down case is higher than that in the spin up case with increasing concentration of Fe in the alloy, for both Ni and Fe partial densities of states, the peak in the spin down case is less sharp and more spread out. Both for the CPA and CCPA the peak corresponding to up spin band has greater height than that corresponding to the down spin band in the case of Ni. This, however, is not so in the case of Fe, where for lower concentrations, the peak corresponding to the down spin band is higher in magnitude. Beyond 20%, however, even in the case of Fe, the up spin band has a higher peak than the down spin band. A comparative study of figures (4.3) - (4.6) will reveal that CPA and CCPA differ mostly in the minority spin band of Fe. This is expected since the disorder parameter $(\epsilon_A - \epsilon_B)/W$ (where W is the band width) is large in the minority spin band. It is well known from earlier work on model systems that almost all the difference between CPA and CCPA arises in this regime. The effect is largest at low concentrations.

In the CPA calculations, magnetic moment of Fe in the alloy decreases from 3.01 μ_B at c = 0.1 to 2.80 μ_B at c = 0.3, while the magnetic moment of Ni ranges from 0.545 μ_B at c = 0.1 to 0.60 at c = 0.3. In 2CPA calculations, the magnetic moment of Fe ranges from 3.0 μ_B at c = 0.1 to 2.73 μ_B at c = 0.3, while that of Ni ranges from 0.54 μ_B at c = 0.1 to 0.59 μ_B at c = 0.3. Figures (4.7) and (4.8) show

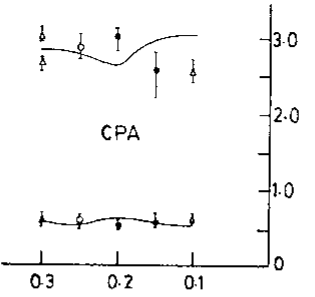

Fig. 4.7 Cocentration against the magnetic moment of Ni and Fe with the experimental data by neutron diffraction (open circle by Shull and Wilkinson 1955; triangles by Collins and Low 1963; and Solid circles by Nishi*et al* 1974).

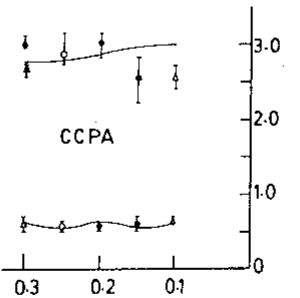

Fig. 4.8 Concentration against the magnetic moment of Ni and Fe with the experimental data by neutron diffraction (open circle by Shull and Wilkinson 1955; triagles by Collins and Low 1963; and solid circles by Nishi *et al* 1974)

respectively the CPA and CCPA results of magnetic moment calculation together with the experimental results of Shull and Wilkinson (1955), Collins, Jone and Lowde (1962) and Low and Collins (1963).

It is found that the concentration dependence of the magnetic moment calculations are in good agreement with the experimental results. The agreement is particularly good for magnetic moments of Fe in the alloy at lower concentrations of Fe. Our results are an improvement over the earlier results of Hasegawa & Kanamori (1971). It is difficult to assess the relative importance of taking a more realistic density of states as compared to the steeple model and the generalisation of the CPA to the CCPA. Since the magnetic moment is an integrated quantity, it is difficult to extricate the effect of improvements on the density of states. In CCPA we take more than one atom into the consideration. In magnetic moments calculation therefore, CCPA should yield better results as the nearest neighbours of an atom play an important part in determining its magnetic moment. This is particularly so for Ni.

CHAPTER V

CONCLUDING REMARKS

In this work we have carried out the application of the Augmented Space Formalism (ASF) to study the spin fluctuations and moment formation in the case of Ni rich $Ni_{1-c}Fe_c$ alloys, particularly for low concentrations of Fe. Previous theoretical works show larger discrepancy between the experimental and theoretical values for low concentrations of Fe in the $Ni_{1-c}Fe_c$ alloy. Thus we have extended the Augmented Space Formalism to the case where the potential itself is calculated self-consistently. Till now the ASF was applied to parameterised Hamiltonians only with great success. In this work, however, we show that in conjunction with recursion method, the Augmented Space Formalism is a generalised method to deal with Hamiltonians which need potentials to be evaluated iteratively.

We have taken the input density of states for the exact d-bands of Ni from the recursion method. This is facilitated by the significant numerical developments made recently in this area. Haydock and Nex (1985) have devised

suitable terminator schemes for the Green function for realistic d-band density of states for the host (Ni in the present case). This gives much better input than in some previous works where the steeple model was used.

In this work, we have also gone beyond the single site approximation. Apart from ICPA we have also done calculations for the CCPA. As we go beyond the single site approximation the magentic moment calculations expectedly improve. Misgivings were expressed with regard to magentic moment calculation via the coherent potential approximation. It was argued that magnetic state of a given atom depends sensitively on the composition of its nearest neighbors. So CPA as a tool for magnetic moment calculation was considered inadequate as it considers single atom with its environment treated as a mean field. CCPA, therefore, expectedly should improve results, because there we at least consider an atom and its immediate environment *exactly* and replace the further away environment by a mean field.

Hasegawa and Kanamori (1972) argue that CPA is a meaningful tool for going into the details of the calculation. When the majority spin band lies below the Fermi level (as in the case of Ni), the magnetic state of each atom is stable since a fluctuation in the magnitude of the magnetic moment is brought in only by a fluctuation in the number of electrons with minority spin, thus the fluctuation

is generally suppressed because it is always accompanied by a change of electrostatic energy. The neutron diffraction experiment done by Collins and Low (1965) indicate that Fe and Co as impurities in Ni may not appreciably disturb the magnetic moments of surrounding Ni atoms. Our calculations indicate that the minority spin density on Ni-sites are most appreciably affected as we go from the CPA to the CCPA. The net result on the magnetisation is small, and of any significance only in the low concentration regime i.e. the so called 'impurity band' regime where model calculations earlier indicated that CPA and CCPA should differ. The magnetisation at low concentrations calculated by the CCPA seems to be in better agreement with experiment. We should, however, not stress too much on this, as the tight binding model calculation should indicate trends rather than really quantitatively reliable estimates.

As future works in this area, need was felt to go beyond the tight binding approximation. For metallic alloys, the self consistent KKR-CPA techniques have been developed. The KKR equations have close resemblance to the tight binding method. The diagonal ε_i term in the tight binding Hamiltonian is replaced by the inverse t-matrix, the off-diagonal hopping term V_{ij} is replaced by the structure function $B_{ij}^{LL'}$, and the Green function by the path operator.

One has to go beyond the single site approximation.

More so if one has to consider the magnetic states of the alloy, as magentic moment on an atom depends on its nearest neighbours. The generalisation of the Augmented Space CCPA to KKR methods has recently been carried out by Mookerjee (1987).

In cases, where the basis is not countable, an embedding technique was developed by Mookerjee and Bardhan (1989) generalising the earlier work by Inglesfield (1981). It is essentially a generalisation of the partition theorem. The Augmented space method then allows us to develop a CCPA procedure in such cases. This work is in progress and will enable us to study systems with random distribution of extended impurities or defects.

Our calculations are at T=0. However, most experimental observations are not at T=0. So it could be interesting to study the magnetic phase diagrams with varying temperatures. This involves the calculation of the Free energy and is a much more difficult propoaition.

Fe has, as we know, both bcc and fcc phases. It could be interesting to study the structural phase transitions of alloys involving Fe. This study will involve estimation of the pair potential and through this the Free energy. This work is being taken up by our group.

REFERENCES

Anderson P.W.,(1969) Phys. Rev. 181, 25

Ahmed M. & Mookerjee A.,(1989) J Phys. *Condensed Matter* (in press)

Baraff G.A. and Schluter M., (1986) J. Phys. C19, 4838

Bishop A.R.& Mookerjee A., (1974) J.Phys. C7, 2165

Butler W.H., (1972) Phys. Lett.39, A203

Butler W.H., (1973) Phys. Rev. B8, 4409

Chandrasekhar S., (1960) *Radiative Transfer* (Dover,New York)

Condon E.U.& Shortley G.H.,(1935) *Theory Of Atomic Spectra* (Cambridge University Press)

Collins M.F. Jones R.V.& Lowde R.D.,(1962) J. Phys. Soc. Japan 17 B-III, 19

Cheney E.W., (1966) *Introduction To Approximation Theory* (McGraw-Hill,New York)

Chihara T.S., (1978) *An Introduction To Orthogonal Polyomials* (Gordon & Breach,New York)

Gray L.J. & Kaplan T., (1981) Phys. Rev. B24, 1872

Haydock R., (1972) *Ph.D Thesis* (University Of Cambridge)

Haydock R., Heine V.& Kelly M.J., (1972) J.Phys. C5, 2845

Haydock R., (1980) *Solid State Physics* 35, (Academic Press:New York)

Haydock R.& Nex C.M.M., (1984) J. Phys. C17, 4783

Haydock R.& Nex C.M.M., (1985) J. Phys. C18, 2235

Hasegawa H., Kanamori J., (1971) J. Phys.Soc. Japan 31, 382

Hasegawa H., Kanamori J., (1972) J. Phys.Soc. Japan 33, 1599

Hubbard J., (1963) Proc. Roy. Soc. A276, 238

Huffner S., Wertheim G.K. & Wernicj J.K., (1973) Phys. Rev.152, 505

Inglesfield J.E., (1981) J.Phys. C14, 3795

Kanamori J., (1963) Prog. Theor. Phys. 30, 275

Kaplan T. & Gray L.J., (1976) Phys. Rev. B14, 3462

Kaplan T. & Gray L.J., (1977) Phys. Rev. B15, 3260

Kumar N. & Jayannavar A.M., (1985) Phys. Rev. B32, 3345

Kumar N. & Jayannavar A.M., (1986) J. Phys. C19, 5513

Kirkpatrick S., Velicky B. & Ehrenreich H., (1970) Phys. Rev. B1, 3250

Low G.G.E. & Collins M.F., (1963) J. Appl. Phys. 34, 1195

Mills R. & Ratanavararaksa R., (1978) Phys. Rev. B18, 5291

Mookerjee A., (1973a) J. Phys. C6, L205

Mookerjee A., (1973b) J. Phys. C6, 1340

Mookerjee A., (1975a) J. Phys. C8, 24

Mookerjee A., (1975b) J. Phys. C8, 1524

Mookerjee A., (1975c) J. Phys. C8, 2688

Mookerjee A., (1979) *Disordered Systems* (Hindustan Publishing Corporn : Delhi)

Mookerjee A., (1987) J. Phys. F17, 1511

Mookerjee A. & Bardhan S., (1989) J.Phys. *Condensed Matter* 1, 509

Müller-Hartmann E., (1973) Solid State Commun. 12, 1269

Nickel B.G. & Krummhansl J.A., (1971) Phys. Rev. B4 4357

Nishi M., Nakai Y. & Kunitomi N. (1974) J. Phys. Soc. Japan 37, 570

Nex C.M.M., (1978) J. Phys A11, 653

Nex C.M.M., (1984) Computer Phys. Commun 34, 101

Seib D.H. & Spicer W.E., (1970) Phys. Rev. B2, 1676 ; 1694

Stocks G.M., Williams R.W. & Faulkner J.S., (1971) Phys. Rev. Lett 26, 253

Soven P., (1967) Phys. Rev. 156, 809

Shull C.G. & Wilkinson M.K., (1955) Phys. Rev. 97, 304

Tsukada M., (1972) J. Phys. Soc. *Japan* 36, 1477

Velicky B., Kirkpatrick S. & Ehrenreich H., (1968) Phys. Rev. 175, 747

Watson R.E., (1960) Phys. Rev. 118, 1036